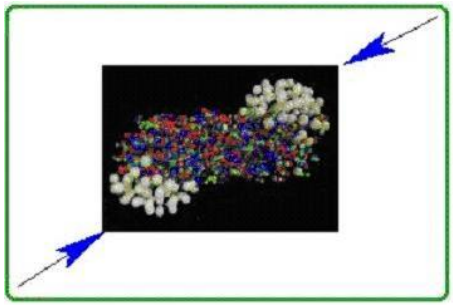

High Energy
High Intensity
Hadron Beams

Proceedings of Workshop on
"DC Current Transformers and Beam-Lifetime Evaluations"
Lyon, 1-2 December, 2004

Edited by A. Peters[1], H. Schmickler[2], K. Wittenburg[3]

1) GSI, Darmstadt, Germany
2) CERN, Geneva, Switzerland
3) DESY, Hamburg, Germany

Abstract

This report contains the final proceedings of the 2nd meeting in the framework of the CARE-HHH-ABI networking, held 1. -2. December 2004, in Lyon, with the subject: "DC current transformers and beam-lifetime evaluations".

Proceedings of the

2nd meeting in the framework of the CARE-HHH-ABI networking

DC current transformers and beam-lifetime evaluations

F-69004 Lyon, Hotel Metropole
01.-02. Dec. 2004

The European Community wants to reinforce the communication between scientific laboratories of similar nature in the field of high energy high intensity hadron beams . For this reason a so called "networking" program has been defined, which over the next five years will join instrumentation experts in order to exchange knowledge on well defined subjects. (CARE-N3 networking for HHH, i.e. for **H**igh Energy, **H**igh Intensity **H**adron Beams). These events are not in concurrence with more general instrumentation workshops like DIPAC or BIW.

The second event of the Work package ABI (advanced beam diagnostic) was proposed by Kay Wittenburg (DESY), Andreas Peters (GSI) and Hermann Schmickler (CERN) with the following topic:

"Beam intensity measurements and lifetime calculations"

The purpose of the event is:

- to review the present technologies available for the measurements of the integral (DC) beam intensity
- to isolate individual physical or technological limitations in the performance of these devices
- to discuss new ideas for those measurements
- to define R&D programs for those new concepts
- to discuss specific algorithms used to calculate lifetimes from the beam current measurements

For these objectives we consider important the experience from the major three European laboratories working with hadron beams (DESY; GSI; CERN) and experience from SNS and BNL in the US (RHIC machine). The experience was complemented by one or two participants from an industrial company (Bergoz Instrumentation)

Participants:

CERN: P.Odier, U.Raich, A.Burns, H.Schmickler, R.Schmidt
SNS: T.Shea
GSI: H..Reeg, A. Peters
Universität Kassel: M.Haepe
DESY: K.Wittenburg, R. Neumann, M.Lomperski, K.Knaack, M.Werner
Bergoz Instruments: K.Unser, J.Bergoz

Contents:

DCCT TECHNOLOGY REVIEW

P.Odier, CERN AB/BDI, Geneva, Switzerland

Abstract

DC Current Transformers (DCCT) are widely used in the world of particle accelerators. Almost all circular accelerators have at least one DCCT installed in order to measure the circulating dc beam current.

The paper describes the principle and the evolution, from basic passive AC Current Transformers (ACCT) to sophisticated DCCTs. Additional features and auxiliary systems are also presented as well as magnetic materials used for the cores and for the shielding. Finally, some problems of integration, their possible solution and the performances currently achieved are addressed.

PRINCIPLE OF ACCTs

An AC Current Transformer (ACCT) consists of a coil wound around a core crossed by the particle beam to be measured, see Fig.1. A signal is generated in the secondary winding by a time varying magnetic flux due to the beam current.

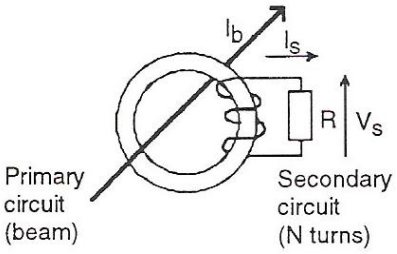

Fig.1 ACCT schematic

Such a device has a low frequency response limited by the inductance of the secondary winding and by the load impedance, corresponding for practical cases to a few kilo Hertz. To overcome this limitation, an amplifier reducing the load impedance and feedback has been added [Ref.1, 2], allowing the extension of the low frequency cut-off to a few Hertz but still not to dc.

PRINCIPLE OF DCCT

The need to measure the dc current arose with the particle accumulators in which the coasted beam stays for days.

The principle of fluxgate magnetometer [Ref.3] has been applied to cover the missing frequency bandwidth of the ACCT [Ref 4, 5]. It resides in the utilization of a magnetic modulator exploiting the non-linear magnetization curve of soft ferromagnetic material. Two cores are fed in opposite phase with a current or a voltage signal according to the chosen configuration. The pair of cores must be carefully matched in order to minimize the induced signal after subtraction. In case of voltage excitation, the generator can be trimmed for each core by means of a balance. The Fig.2 shows the effect of a voltage modulation driving the cores into saturation. The frequency spectrum of the modulation current presents only odd harmonics when the BH curve is symmetrical with respect to the B and to the H axis; this is the case when the beam current is equal to zero. In contrary, a non-zero beam current causes an asymmetry of the BH curve and as a result the appearance of even harmonics and in particular of the second harmonic.

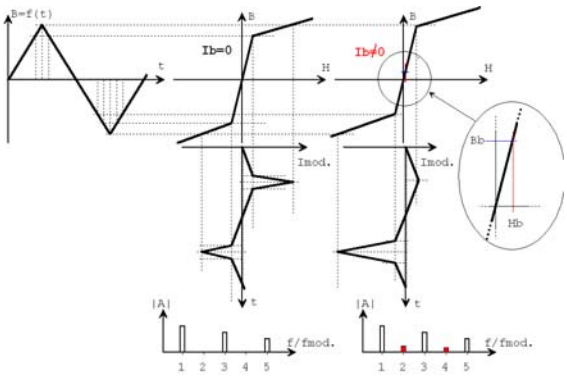

Fig. 2 Production of even harmonics

The magnetic modulator can be seen as a magnetic mixer shifting the beam signal frequency spectrum by twice the modulation frequency.

As seen above, the excitation generator can be either a voltage or a current generator, producing a rectangular, triangular or sinusoidal waveform. The choice of the modulation frequency depends on the magnetic material's permeability variation with frequency, a few hundreds Hertz for crystalline material and a few kilo Hertz for amorphous materials. The essential features for a modulation generator are either high current or high voltage capabilities to saturate well enough

the cores as well as frequency spectrum purity, the latter being not easy to achieve with highly non-linear load.

The extraction of the useful signal, the second harmonic, can be seen as the reverse operation of the frequency shift made by the magnetic modulator. Different options exist:

- synchronous detector
- resonant filter + detector or sample and hold
- detector of phase shift in saturation passages

The synchronous detector performs the product of the raw signal with a signal having the right phase and a frequency twice the modulation frequency.

The DCCT is often called zero-flux DCCT because of a feedback current cancelling the flux induced by the beam current. The aim is to increase the linearity range (to more than 6 decades) and to reduce the recovery time allowing the observation of low intensity beam after the passage of a high intensity one. The condition to achieve this goal is that the feedback current should be always equal to the beam current, therefore no interruption is allowed.

The frequency bandwidth of the magnetic modulator is limited to less than half the modulation frequency in order to avoid aliasing. Thus the signal induced in a third core is added to the dc signal to generate a common feedback. This additional part extends the high frequency cut-off of the overall transformer to some tens of kilo Hertz. The overall principle schematic is shown in Fig.3.

A demagnetization circuit insures the B-H curves to be well centred. The process avoids the memory effect and reduces the offset. This circuit should be activated, without any beam, at power on and on request.

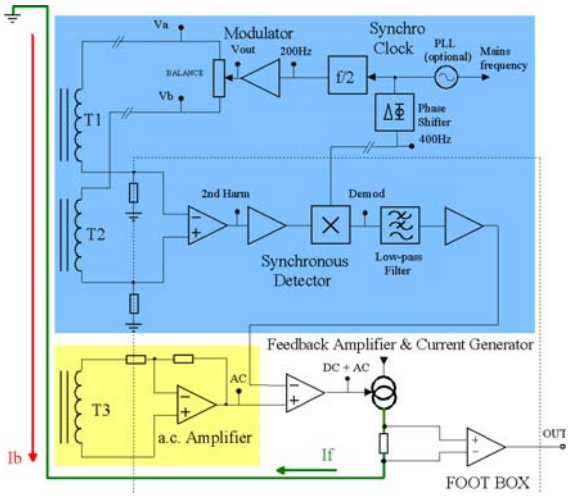

Fig.3 DCCT general schematic

SIGNAL TREATMENT

Diverse signal treatments, performed either by hardware or software, can be applied to DCCT raw output signal.

- Ripple suppression, reduction of the modulation's harmonics
- Base line restitution, acquisition of the perturbing signal for subsequent subtraction, only valid for accelerators with short cycle duration, a few seconds
- Offset suppression, acquisition of the DCCT signal in absence of beam then subtraction
- ß Normalization, transformation of the DCCT's output signal proportional to the beam current into a signal proportional to the number of circulating charges

MAGNETIC MATERIAL

The magnetic material used for the dc core should be carefully chosen to gain the best sensitivity.

The criteria are the following:

- high magnetic permeability μ (>50000)
- low hysteresis losses, proportional to the area of the hysteresis curve
- low coercitice field, H_c ~ 1A/m
- Low eddy current losses, high electrical resistivity, lamination, strip-wound core, thickness of 10 to 50mm
- Low magnetostriction (change of physical dimensions when subjected to a magnetic field and conversely, source of noise)

- Minimum Barkhausen noise (related to magnetic domains structure and dimension)
- Good temperature stability

Three group of soft magnetic material are considered:

- crystalline, NiFe(Mo) alloy
- amorphous, TM alloy
- nanocrystalline, FeSIB alloy

INTEGRATION ISSUES AND POSSIBLE SOLUTIONS

DCCTs are sensitive to HF interferences due to RF systems and to beam structure, particularly to dense bunches. A good screening applied to the monitor, to the cables and to the boxes housing electronic prevent this effect. Capacitors disposed around the ceramic gap reduced the RF field emitted by the beam as well as the longitudinal impedance.

DCCTs are also susceptible to magnetic perturbations due to the surrounding equipment (dipoles, multipoles, power cables, power transformers, vacuum pumps, etc.). Magnetic shielding reduces these perturbations. The shielding effectiveness is improved by a multi layer configuration. The inner layers are made of high permeability material while the external one is made of high saturation material.

Radiation resistance of the front end electronic can be an issue for instruments placed in accelerators. The solution is to move away the electronics when possible, or to protect it with concrete and iron shielding. A wise choice of materials and components is recommended to insure the monitor perennity.

When heating the transformers during vacuum bake-out the core temperature should not exceed ~60ºC, a temperature far below the Curie temperature in order to avoid damage. A water-cooling placed inside the DCCT around the bake-out jacket presents an efficient solution.

PERFORMANCES

Hereafter are listed the standard performances achieved by DCCTs.

- Full scale: any range from 10mA to 100A
- Resolution (S/N=1): typically 1 - 2µA (rms value for 1 s integration time)
- Frequency bandwidth: DC to ~ 50 kHz. Although often deliberately limited for noise reduction
- Temperature dependence: ~5µA/ºC
- Accuracy: ±500ppm + resolution, the main limitations being the calibrator and the monitor LF noise

CONCLUSIONS

The DCCTs are widely used; almost every circular accelerator has at least one device installed.

There is a demand to improve the performance in terms of resolution and stability i.e. reduction of the temperature dependence. Advancements are to be made to susceptibility to beam structure with high density bunches.

The test of new promising magnetic materials is not easy due to difficult procurement for small quantities.

Significant improvements are made in the domain of fluxgate magnetometer for space applications, can these progress benefit to DCCT [Ref.8]?

REFERENCES

[1] R.Webber, “Charged particle beam current monitoring tutorial”, Beam instrumentation workshop, Vancouver, Canada 1994

[2] G.Gelato, “Beam current and charge measurement”, Beam instrumentation, ed. J.Bosser, CERN-PE-ED 001-92

[3] K.Unser, “Beam current transformer with DC to 200MHz range”, IEEE Trans.Nucl. SCI. NS-16, June 1969, pp. 934-938.

[4] K.Unser, “The parametric current transformer, a beam current monitor developed for LEP”, CERN SL/91-42, 1991

[5] W.Geyger, “The ring-core magnetometer-A new type of second-harmonic flux-gate magnetometer”, IEEE Transaction on magnetics, 1962

[7] P.Kottmann, “Theorical and experimental investigation of magnetic materials for dc Beam Current Transformers”, CERN PS/BD/Note 97-06

[8] W.Magnes, D.Pierce, A.Valavanoglou, J.Means, W..aumjohann, C.T.Russell, K.Schwingenschuh, G.Graber, “A sigma–delta fluxgate magnetometer for space applications”, W Magnes et al 2003 Meas. Sci. Technol. 14 1003-1012

EXPERIENCE WITH INTENSITY MEASUREMENT PERFORMANCE LIMITATIONS AT CERN

U. Raich, CERN AB/BDI, Geneva, Switzerland

Abstract

Since the dismantling of LEP no storage rings, making lifetime measurements necessary are operated at CERN. Nevertheless beam intensity measurements are extensively used in the transfer lines between the different accelerators as well as in the accelerators themselves. The operations crew has provided information on where they see performance limitations of the current measurement systems, possible improvements and requests for additional resources.

The paper first gives an overview of the different types of beam current measurements available in the PS and SPS complex today and then describes shortcomings that have been observed.

SYSTEM OVERVIEW

Figure 1 shows all beam current measurements available in the machines of the PS complex. Depending on the beam type different transformer types and readout electronics is used.

In the transfer lines from Linac-2, (proton Linac) to the PS Booster (PSB) and from Linac-3 (lead ion Linac) to LEIR the beam has a length of several hundred µs (~200 µs in the case of Linac-2 and up to 500 µs in the case Linac-3) and fast sampling ADCs followed digital signal treatment a integration are used (transformers shown in magenta). Beam intensities have typical values of 180 mA for Linac-2 and 20 µA for Linac-3.

After multi-turn injection into the Booster, bunching and acceleration, the bunches have a typically lengths of several tens of ns and analogue integrators are used.

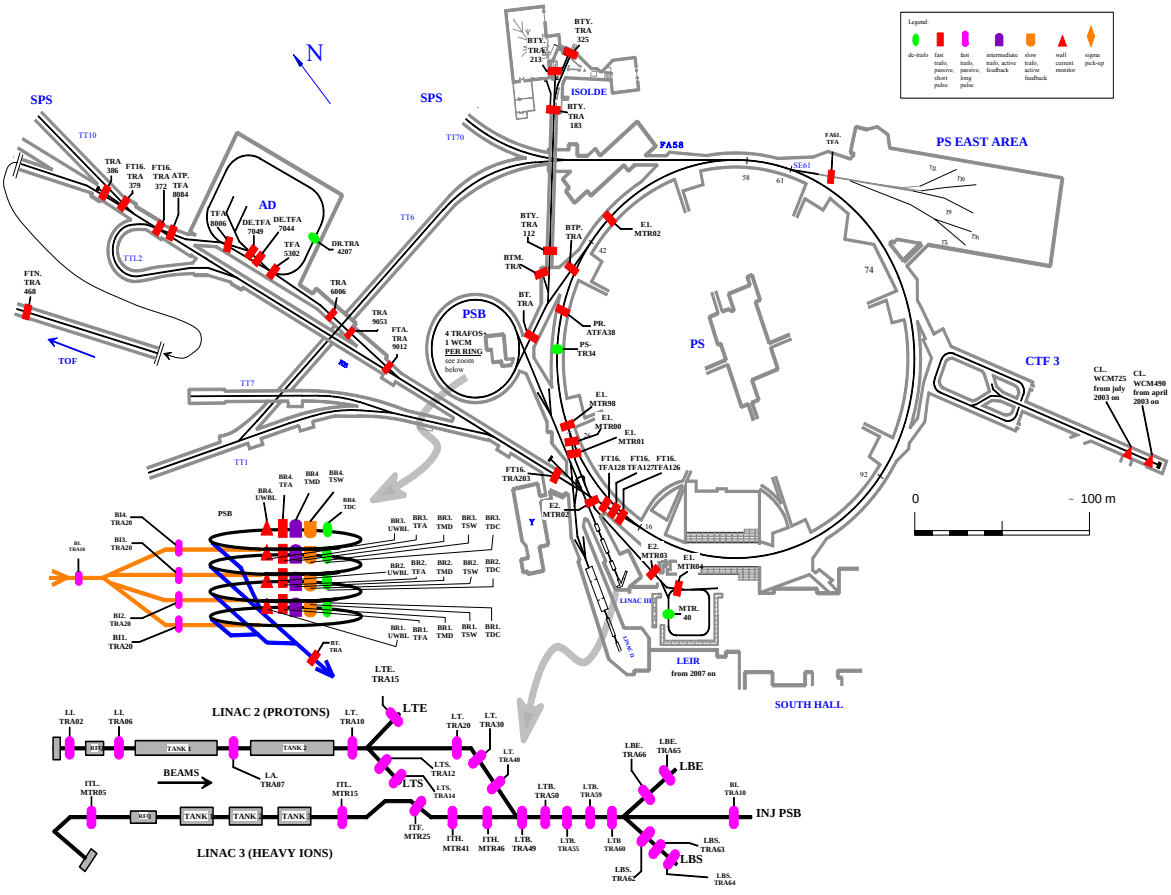

Figure 1: Overview of Beam Current Transformers in the PS complex

Since many of the transformers see vastly different intensities depending on the accelerator cycle (e.g. proton vs ion cycles) a multi-gain amplification system is used (transformers marked in red).

In the circular machines the beams stays for 1-2 s which makes DC current detection necessary (transformers marked in green).

TRANSFORMERS IN THE LINACS

The main problem seen on the Linac-3 transformers is due to the very low intensity ion current resulting in very high amplifications needed in the preamplifier chain. The transformer signal sits on low frequency noise induced by nearby pulsed elements. In order to reduce these effects an analogue baseline restoration is performed by subtracting a ramp signal whose slope must be manually adjusted. In addition a precise current pulse for calibration purposes is injected just before the arrival of the beam.

As can be seen from the trace, the baseline restoration is not perfect and measuring the baseline with subsequent baseline subtraction would be preferable. Unfortunately this would however need a bigger dynamic range for the ADC which is currently limited to 8 bits with only 2kBytes of associated memory. In the near future we foresee to replace the ADCs by 12 bit models having bigger attached memories.

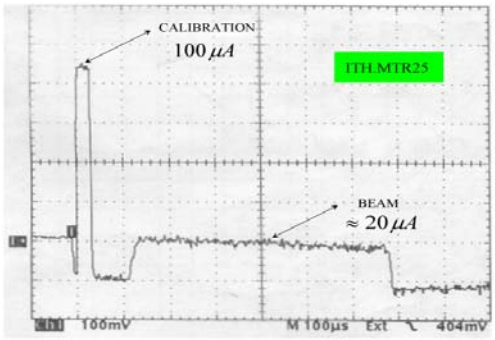

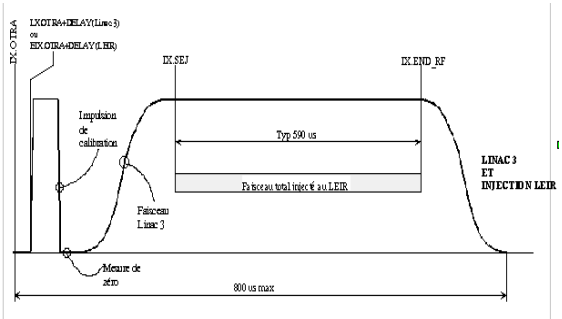

Figure 2:

a) typical oscilloscope trace from a Linac-3 transformer

b) additional signals used for intensity calculations

For very low intensity beams electromagnetic interference constitutes a big problem which can only be resolved through very careful shielding and great care in the use of ground connections.

DC CURRENT TRANSFORMERS

There is at least one DC current transformer (DCCT) in each of the circular machines measuring the intensity of the circulating beams. This transformer is use to observe losses down to the percent level.

When producing beam for the Antiproton Decelerator (AD) the particle bunches are compressed in time (fig 3).

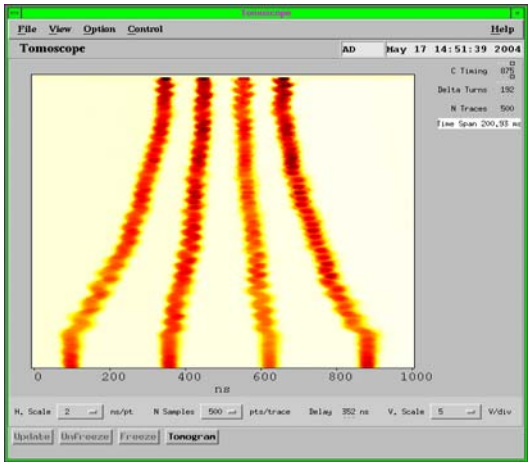

Figure 3: Batch compression of AD beams

When observing this beam in the PS using its DCCT a slight dip in the intensity is observed, this is due to an instrument effect. Figure 4 shows the result of the current measurement. The upper trace represents the plot seen on the control system while the lower trace is zooming in to the critical area.

Changing the distance between bunches and leaving a bigger hole between each batch of 4 bunches modifies the frequency content of the transformer signal. The revolution frequency becomes more visible. This upsets the low frequency amplifier used in the feedback chain of the DCCT electronics.

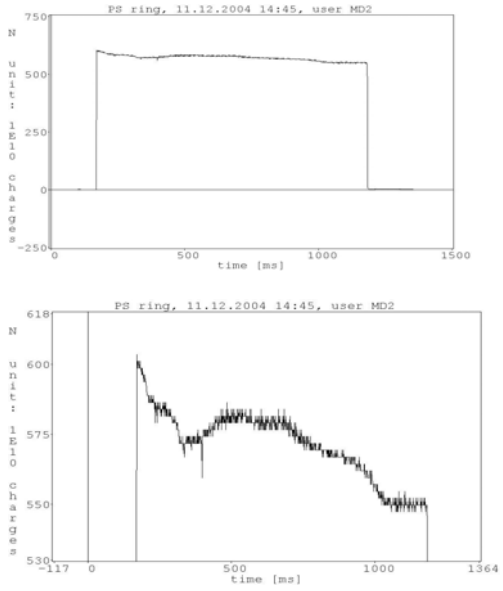

Figure 4: Anomalies in DC current measurements during batch compression.

RELATIVE MEASUREMENTS

When increasing the beam intensities for high current operations like CERN's new neutrino program (CNGS) it becomes more and more important to control possible losses. Relative current measurements allow pinning down the location where such losses occur.

.Fig. 5 shows the location of current transformers along the accelerator chain. It will be important to be able to compare measurements between injection transformers into the Booster, its DCCTs, the transfer line transformers and the DCCT in the PS in order to determine how much losses come from

- the multi-turn injection into the Booster
- the acceleration in the Booster itself
- the ejection process
- the recombination process
- the transfer to the PS
- the injection process into the PS

Cross calibration between different transformers would be necessary but is very difficult to accomplish. For the moment absolute calibration is used (see fig 2) but results depend on differences in multiple gain amplifiers, different coupling of the calibration signals into the transformers, long cables from the control electronics to the device in the machine and EMC problems.

CONCLUSIONS

- Generally low intensity beams cause more problems to the instruments but are less interesting to operation.
  (low freq. EM problems)
- Problems of relative calibration of transformers for loss measurements
- Lack of a transformer measuring many turns at injection. The DCCT sees the injected beam only after around 100 ms due to bandwidth limitations.

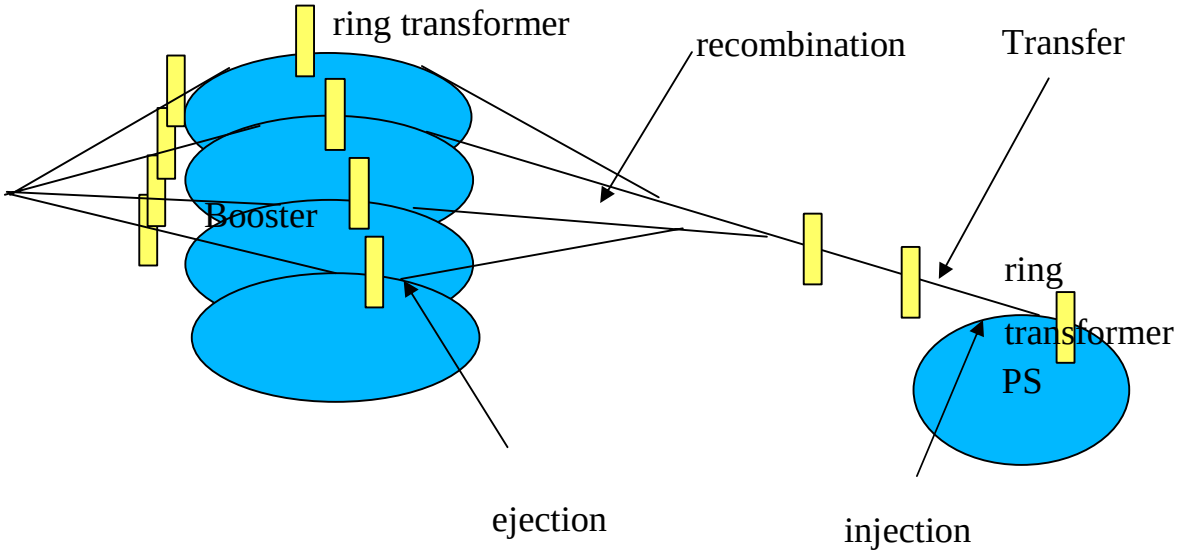

Figure 5: Relative current measurements

Performance Limitations of the DCCTs at GSI

Hansjörg Reeg, Gesellschaft für Schwerionenforschung,
BT/SD, D-64291 Darmstadt

Development of the DCCT for the SIS18 at GSI

The objectives for the development in 1987 were:
- high resolution
- low noise
- beam currents ~mA

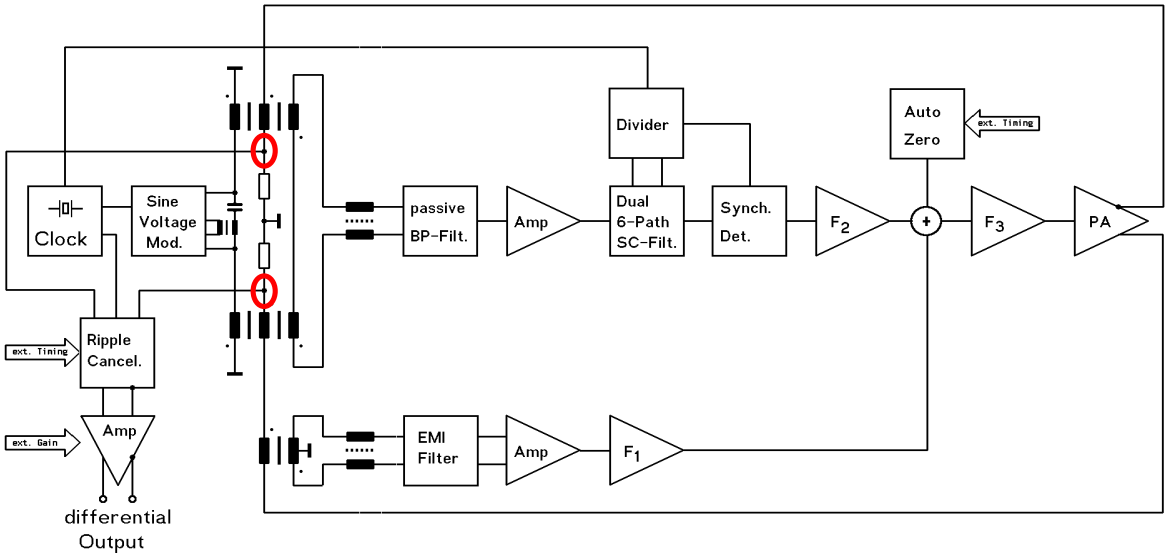

Figure 1: Block diagram of DCCT front-end

In Fig. 1 the scheme of the DCCT can be seen, at the red circle the following equation is valid: $U_{diff} \sim I_{beam}$, the parameters are: $U_{diff} / I_{beam} = 16.66$ V/A, the dynamic range of this system is around 100 dB.

To suppress the ripple caused by the sine voltage modulator, a special electronics was developed, which action is shown in Fig. 2 (vertical axis: 25 µA/div) – on the left side the original ripple, on the right side with ripple suppressor.

A problem of building DCCTs is always the core material, which differs from one production batch to the next, as can be seen in Fig.3, where two hysteresis loops of different material are presented. We use **A; B** was delivered by VAC (Vacuumschmelze, Hanau, Germany) in a 2nd batch, the ordering specification for both cores were identical!

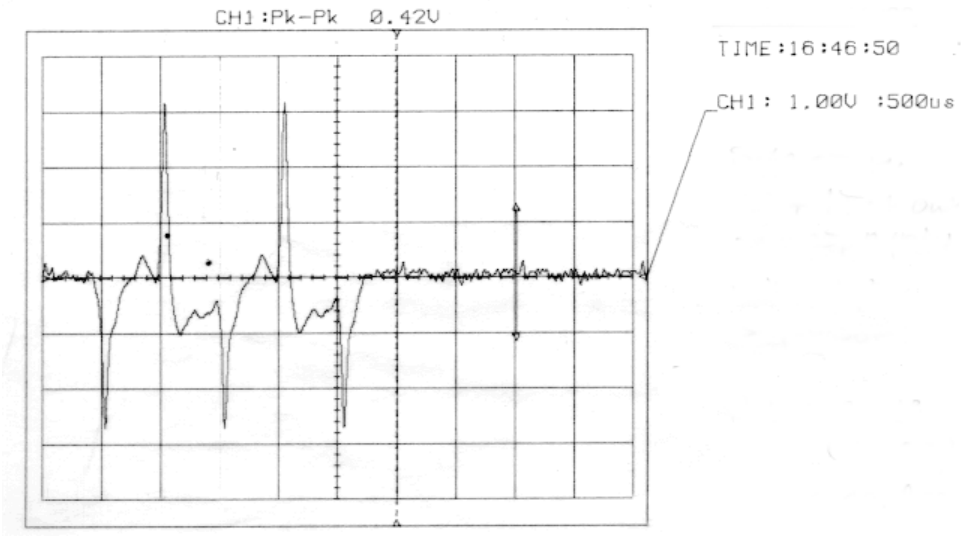

Figure 2: Effect of ripple suppressor, see text

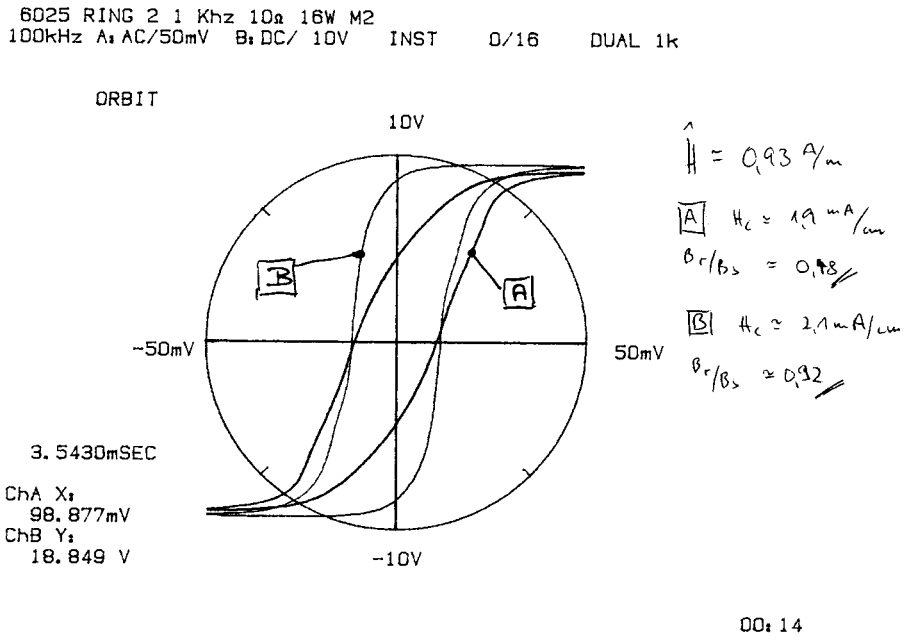

Figure 3: Typical hysteresis loops (from development logbook)

More detailed information on the DC control loop can be found in Fig. 4, where the open loop Bode diagram is shown. The combined system transfer gain function is realized by superposing the DC channel with an AC channel at a crossover frequency of about 6 Hz. In Fig. 5 the DCCT system for SIS18 (left side) as well as the built-in system in the ESR are shown together with some important parameters.

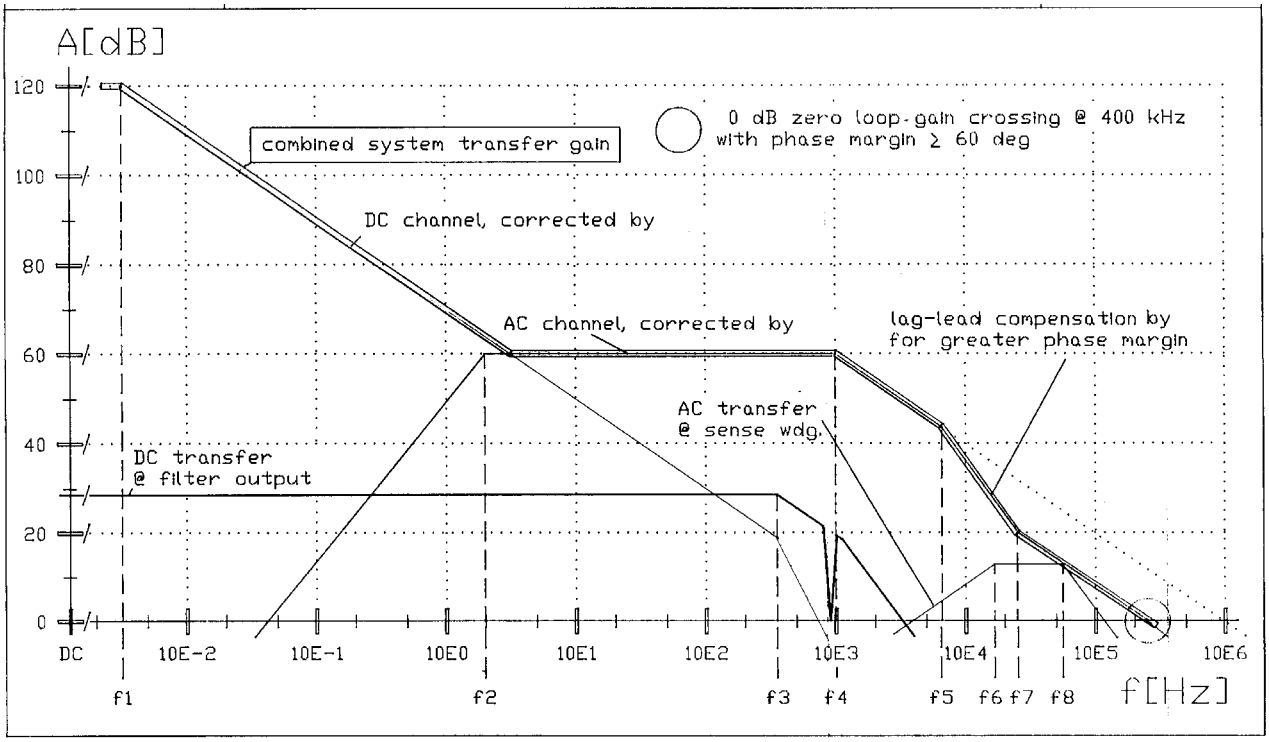

Figure 4: Open loop Bode diagram of the DCCT control loop

•Aperture: DN200CF
•Length: 600mm
•Ceramic gap, resistive coating on inner surface
•Mumetal ® magnetic shield, double-layer
•Toroids separated by shielding rings reduces ripple cross-talk

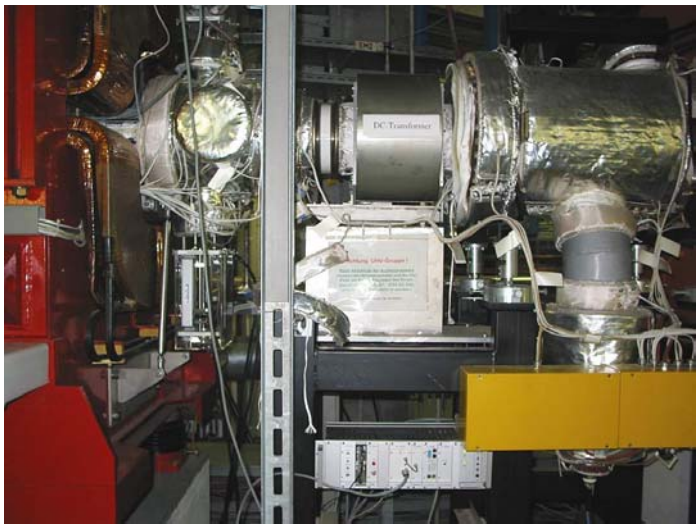

•Remote electronics control/ADC placed outside tunnel
•Locally mounted front end
•SIS/ESR: upgraded with V/f-converter output, fixed range 1 MHz / 20 mA
•ESR: influence of Quad fringe field is corrected by Hall probe input

Figure 5: DCCT for SIS18 (left side) and the ESR at GSI

DCCT Specifications

The specifications of the GSI DCCTs based on the ususal 3-core scheme can be found in the following table:

Dimensions of toroids:	264 x 284 x 10 mm
Magnetic ribbons:	Vitrovac 6025 F, 25 µm
Winding scheme:	N_{loop}=12, N_{DC}=16, N_{AC}=96, N_{mod} =16
Main control loop:	Current ouput, burden resistance 200 Ohm
Sub control loops:	Peak modulation current, AutoZero
Modulator type:	Sine voltage, avalanche capacitor
Modulation frequency:	987.5 Hz
Peak excitation field:	~ 20 A/m
Crossover frequency DC/AC channel:	~ 6 Hz
Open loop gain at DC:	> 120 dB
Open loop-0 dB crossing frequency:	~ 1.2 MHz (~ 0.4 MHz before upgrade)
Signal transmission, toroids to front end:	differential, twisted pair lines
Cable length, toroids to front end:	2.5 m, limited by capacitive loads
Shunt impedance, min. @ DC:	~ 2 kOhm
8 Ranges:	± 300 µA to 1 A DC f. s, (1...3...10)
Winding scheme:	crossed-differential, unchanged by range switching
Amplification error:	< 0,1 % (for I < 20 mA)
Linearity error:	< 0,1 % (for I < 20 mA)
Overrange margin @ DC:	~ 20 % f.s.
1/f-noise corner frequency:	~ 2 Hz
Temperature coefficient:	~ 5 µA/°C
Zero error, SIS type:	± 10 µA with AutoZero on, (± 2.5 µA before upgrade)
Zero error, ESR type:	± 2.5µA
Ripple cancellation, SIS type:	by ADC-RAM-DAC system, reduction ~ 32 dB
Ripple cancellation, ESR type:	by 2f-synchroneous sampling at zero crossing point
Current resolution, SIS type:	20 µApp @20 kHz bandwidth (~ 5 µArms), S/N = 1
Current resolution, ESR type:	5 µApp @20 kHz bandwidth (~ 1 µArms), S/N = 1
Output bandwidth:	DC - 20 kHz (small signal, 1st order LP filtered)

Operations at beam currents with lower level

For beam currents at lower levels the GSI DCCTs work as expected. The noise level is dominated by the Barkhausen effect. In Fig. 6 example measurements at SIS18 are presented. A whole SIS cycle from injection to extraction is displayed and the lower picture shows the calculated particle numbers during the cycle taking into account the RF, respectively the revolution frequency of the beam.

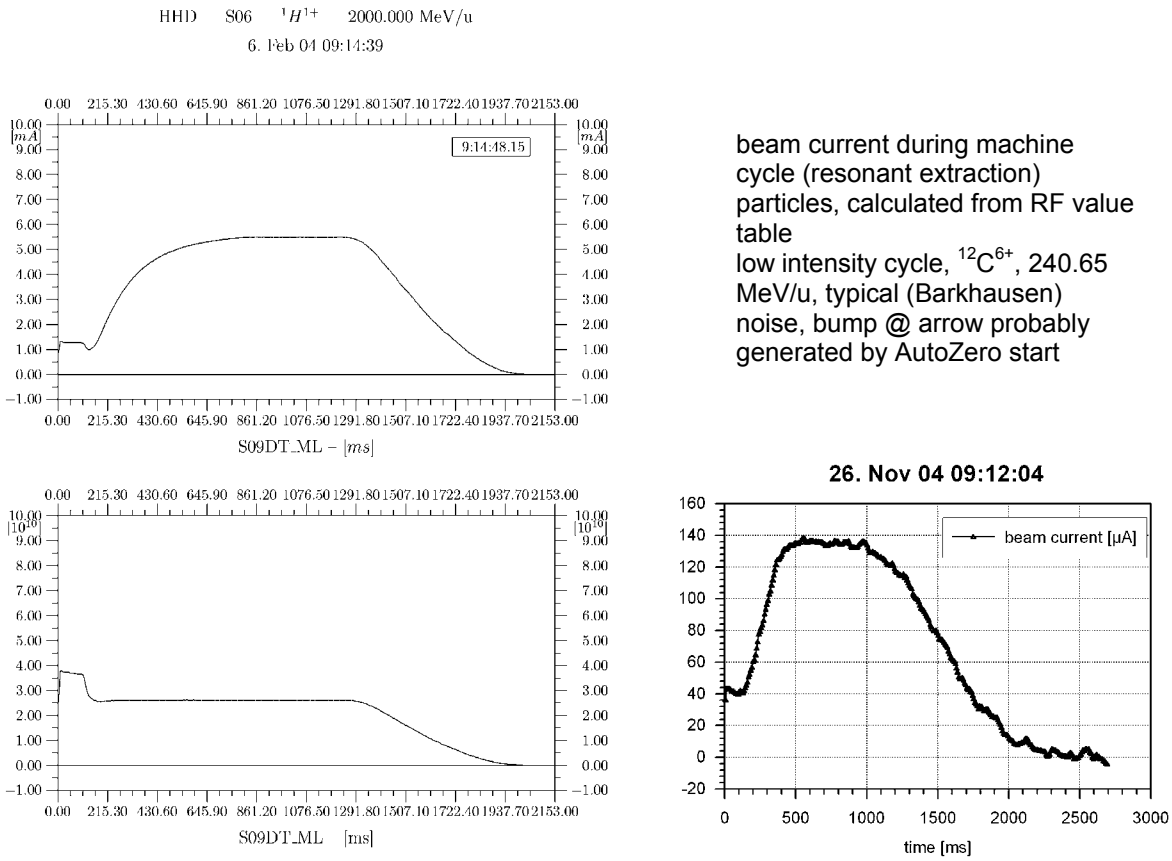

Figure 6: Example measurements with the SIS18 DCCT with a maximum current at 5 mA

The parameters for the standard operation at SIS18 are as follows:f_{rev} = 210 .... 1400 kHz

- h = 4multiturn injection (<40 turns)
- resonant extraction, max.10 sec
- cyclic operation of different settings (ion, energy, ...)
- cycle length max. 30 sec
- ~ 100ms gap without beam between consecutive cycles

Operations at higher beam currents

At higher beam currents at about 70 mA and f_{bunch} ~ 1.2 MHz (almost included within the acceleration ramp) the feedback loop of the DCCT looses control. The loop starts to oscillate and mostly it gets back control, see Fig. 7 for an example. But the question remains: Did it settle to the correct working point?
For the high current operation of the SIS18 an upgrade program for the DCCT was therefore started.

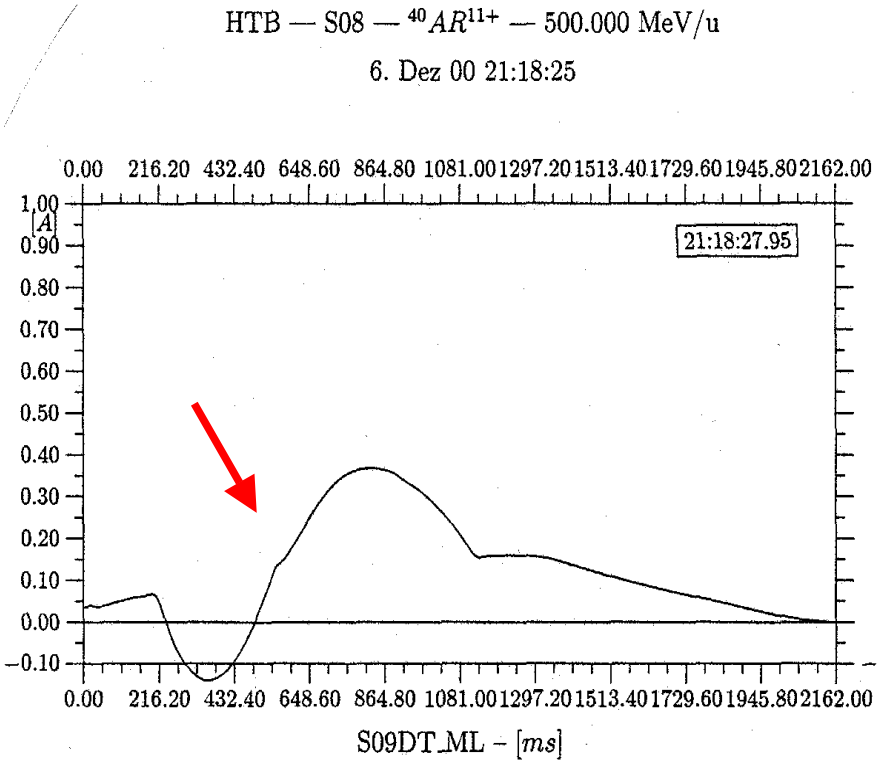

Figure 7: Example measurement with malfunctioning control loop

The following improvements were performed:

- Improved RF filters on sense inputs
- Updated control loop electronics
- Faster operational amplifiers in correction and current driver stages
- Modified lag-lead compensation
- 0dB gain crossing point now ~1 MHz
- Installed local RF bypass around DCCT core stack

Unfortunately the noise of the DCCT increased by a factor of 4, the reason for that is yet unknown. As a second improvement attempt, the installation of a capacitive gap bypass was tried, but it showed to be almost ineffective! The results of all this improvements are shown in Fig. 8

Requirements for the future

The SIS18 will reach the space charge limit for Uranium in 2006 to 2008. Thus, the peak bunch current will be clearly above 1 A. A practical solution for the current measurement system is to rely on Bergoz Instrumentation and their new DCCT version (NPCT) during a long machine shutdown in 2006. For the FAIR project (SIS100/300) the bunch frequencies will be halved and the dynamic range will be extended once more: from currents in the µA region until > 10^{12} U^{28+} resulting in peak bunch currents of 150 A. In addition, the storage times in new rings will be prolonged enormously, which will cause problems with the zero drift.

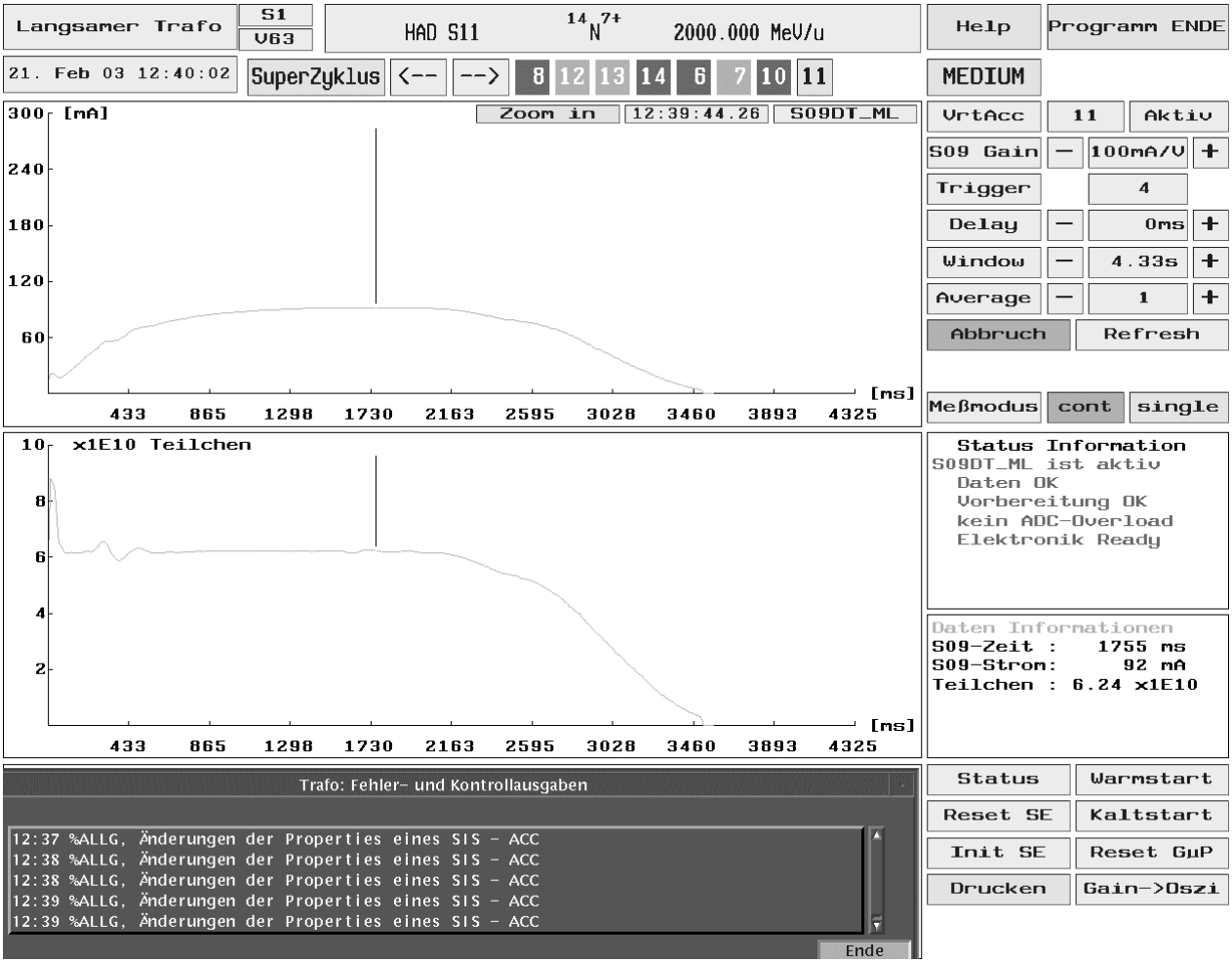

Figure 8: Measurement with the improved DCCT

Acknowledgement

The DCCTs and other GSI current transformers species were developed and built in a fruitful joint work with Norbert Schneider.

Lifetime Calculations at DESY: Improving the reaction time of the measurements in the presence of low frequency DCCT noise.

CARE-HHH-ABI Networking Meeting
1+2 Dec 2005, Lyon

Klaus Knaack, Mark Lomperski

1 Introduction

Beam lifetime calculations are performed at DESY for the DORIS, PETRA and HERA accelerators/storage rings. They are at present based on beam current measurements with PCTs (DCCTs) from Bergoz [Ref.1]. In steady state, good lifetimes are 20 hours (for electron and positron operation) and up to thousands of hours for protons. For accelerator operations, a fast, real-time display of the lifetime is vital. The algorithm currently in use tends to smooth-out sudden changes in the beam lifetime. Our attempts at providing a real-time lifetime display are collected here. The limitations set by low frequency noise (drifts) of the DCCT output are described.

2 DCCTs at DESY

The following table shows the specified ranges and resolutions of the DCCTs for an integration time of 1 second. Because of the long proton lifetime, the PCT chosen for HERA p has a very high resolution.

Accelerator	Range	Resolution
HERA-e	Up to 200 mA / 20 mA/V	< 5 microA
HERA-p	Up to 200 mA / 20 mA/V	< 0.5 microA
PETRA	Up to 200 mA / 20 mA/V	< 5 microA
DORIS	Up to 400 mA / 40 mA/V	< 2 microA

Photos of the installation are seen in Figures 1 and 2.
The Bergoz PCT equipment provides a DC voltage between 0 and 10 V. This beam-current proportional voltage is digitized by Agilent 3458A digital volt meters (8 ½ digits) at a rate of a few Hz. The values are read-out over GPIB.

3 Limitations in our Algorithm

The algorithm currently in use for lifetime calculations was written by W.Schuette [Ref.2]. For a complete discussion of the algorithm, please consult the reference. A qualitative discussion is included here.
The algorithm was developed for the large dynamic range needed for the HERA-p ring, where a good lifetime can be many thousands of hours, but one also needs to measure

lifetimes of less than one hour. A buffer of measured beam currents is kept and a least-squares fit to a line is made to find the slope of the beam current versus time. A history of up to more than 1 minute is needed to measure long lifetimes. If the lifetime changes suddenly (e.g. suddenly drops) then the complete history buffer cannot be used, and only the last few points are taken. As each new value is taken, a check is made if the value is "consistent" with the lifetime just calculated, or if a change has taken place. A decision must be made of how far back in the history points should be included for the fit.
For optimal use of the algorithm, one needs to set the limits for changes in the beam-loss per unit time / the lifetime. A problem with the algorithm is that lifetime changes can be missed by the data-check, resulting in too long a history buffer being used which smooths-out a sudden change in the lifetime. In fig. 3 is shown an example of this effect.

4 First Approach: A Lifetime in 0.5 sec

Our first approach was to digitize the DCCT output voltage at a very high rate (> 10 kHz) and fitting a line to a data set of 0.5 seconds. The integration time of the DVM is much shorter, increasing the noise of the signal, but with large enough sampling rates we found that the statistical error in the determination of the slope of the beam-current versus time to be adequate to measure lifetimes up to 10 to 20 hours.
What we found was that the RMS fluctuations of the calculated lifetimes were 5 to 10 times larger than the statistical error in the fit. Looking at FFTs of long data sets (10 minutes) we found low frequency noise (< 0.1 Hz) in the signal. Looking at the beam-current versus time, we observe what looks like drifts of the signal – quasi stable values with sudden jumps. Examples are shown in Figures 4 and 5. These drifts were also observed with no beam in the accelerator.

Our conclusion: due to the low frequency noise/drifts of the DCCT output voltage, it is not useful to fit the beam current on data sets of less than 2-3 seconds. We are back to our original problem. The solution is to find an improved algorithm to decide when the lifetime has changed.

5 New Approach: The SLAC PEP-II Algorithm

In informal discussions with Diagnostics Colleagues at SLAC (namely Alan Fisher) on DCCT based beam diagnostics, we learned about the algorithm used to calculate the beam lifetime at PEP-II. The decision to shorten the length of the buffer for the fit is made based on the value of the chi^2 of the fit. Simply put, the Chi^2 for a fit to a line is made for long time buffers, and if the value of the Chi^2 is above a threshold, then the buffer length is shortened.
This algorithm could be easily programmed, and easily compared to the older algorithm.

6 Comparison of Algorithms

To facilitate a comparison of algorithms, and also to tweak parameters and study the effects on “response-time” to lifetime changes and sensitivity to noise, a special data set was prepared. The beam current data was taken during a standard DORIS run with stable lifetime. Lifetime “changes” were then added: a sudden drop in the lifetime and sudden recovery, sudden beam loss, and noise in the form of spikes. The lifetimes calculated with different algorithms can in this way be compared with “controlled” input data. In Figure 6 are shown plots of the lifetime breakdown and recovery, calculated with the “old” and SLAC algorithms. The Chi^2 algorithms shows much better time response.

7 Summary

DCCTs are a standard diagnostic for beam current and lifetime measurements t DESY. Slow response of our lifetime algorithm necessitated studies of the noise of the DCCT output voltage. Low frequency noise (or drifts) were found which makes it impossible to base a fast-reacting beam-lifetime calculation on short data samples (< 1 sec). Data must be collected over longer periods and the loss rate determined from the slope. Implementation of the algorithm currently used at SLAC brought improvement over the algorithm we are currently using.

REFERENCES

Ref 1: DCCTs, Bergoz.

Ref 2: W.Schuette, PAC ,93.

Ref 3: Alan Fisher, SLAC, private communication

Figure 1: The HERA-e DCCT installation: a simple construction with water cooling.

Figure 2: The HERA-p DCCT installation: a more complicated structure with heat sinks.

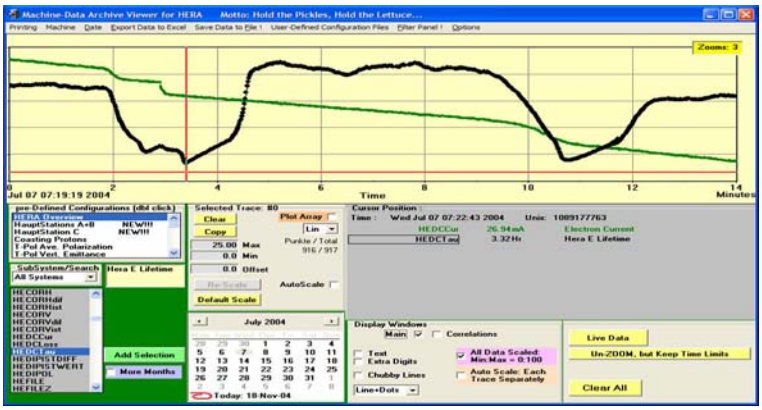

Figure 3: Archive data from HERA-e. Two short lifetime breakdowns are shown. The calculated lifetime shows a very slow response.

Figure 4: Beam current versus time measured in DORIS over one minute.

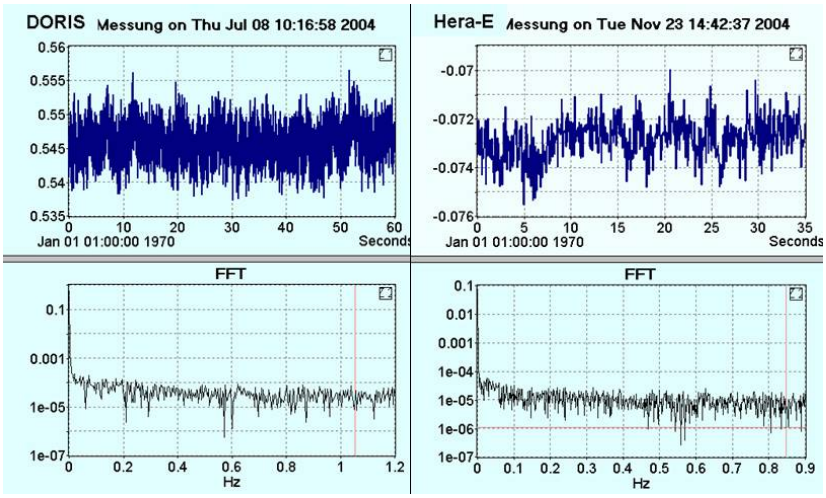

Figure 5: Beam current versus time measured in DORIS and HERA-e over 30 seconds.

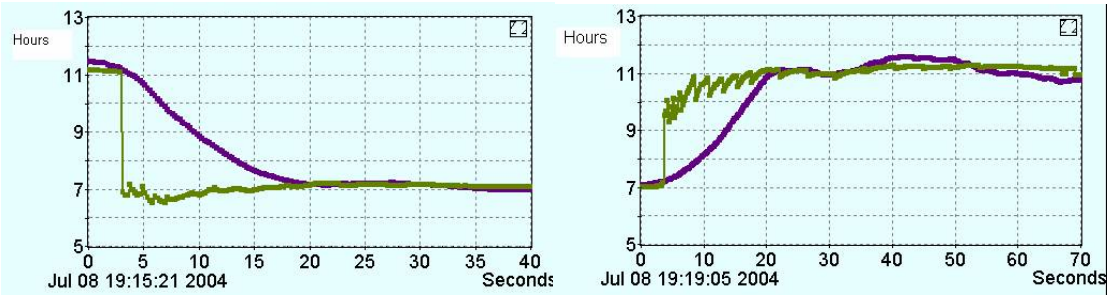

Figure 6: The “controlled” lifetime breakdown and recovery in the special DORIS data set, calculated with “old” and SLAC-Chi^2 algorithms. The Chi^2 algorithm reacts much more quickly to the sudden lifetime change.

Comparison: ACCT-DCCT

The 2nd meeting in the framework of the CARE-HHH-ABI networking
1-2. December 2004 in Lyon

Reinhard Neumann, MDI-4, DESY
reinhard.neumann@desy.de

At the DESY accelerator complex, different **C**urrent Transformers are installed to measure beam current. A modular, PC-based single bunch instrumentation system is presented. AC- and DC current measurements for HERA p are compared, especially to get an indicator for unbunched (coasting) beam.

DCCT´s at DESY

For DC current measurement at the DESY accelerators DCCT´s from Bergoz Instrumentation are mounted. The PCT and MPCT are used on most particle accelerators in the world to measure the average beam current. More information about DCCT technology are presented in other talks of this workshop.

ACCT´s at DESY

At the DESY accelerators, inductive pickup stations deliver suitable signals for single bunch/single pass current monitoring.The bunch intensity measurement is complementary to the precision monitoring of IDC . In connection with other instrumentation this 'AC-current' monitor is used for various diagnostics and applications, such as luminosity and background counting at HEP experiments, measurement of the transfer efficiency between transportline and storage ring, timing calibrations (kicker timing, 'first' bunch timing, etc. . .), proton injection optimization (bunching),...

A PC-based Bunch Current Monitor

As all storage rings at DESY (HERA, PETRA and DORIS) now operate with a similar *interbunch spacing* – multiples of 96 ns – a modular design of the bunch current monitor is applied. The analog input of the apparatus is fed from an *inductive pickup* station , which delivers a *pulse signal* proportional to the bunch current. The bunch currents are measured by *digitizing* the level of each 'bunch pulse'. Therefore the signal has to be prepared, i.e. pulseforming, amplification and sampling, which takes place in the analog signal processing section. The trigger signals, which are needed for the Track&Hold sampling stage and the ADC digitizer, are derived from an external, bunch synchronous timing system. Fig. 1 gives an overview on the hardware.

The analog and trigger signal sections are designed in-house, while for the digitalization a commercial plug-in PC-board is used.

ANALOG SIGNAL PROCESSING

The analog signal path is bandlimited, and mainly defined by the *pulse-forming low-pass filter*. The impulse response of all the linear sections together (pickup, cables, pulsefilter and amplifier) is chosen to form a pulse proportional to the bunch intensity; which on the one side is long enough to be sampled by the following T*rack&Hold* amplifier stage, but on the other side is small enough not to decay into the following 96 ns bucket (AnalogIN *[FWHM]* = 35 ns . As the electron/positron - as well as the proton-bunches are much shorter in time, this linear analog path acts like an integrator. The processed pulse signal is proportional to the total charge of each bunch.
The other signal processing components are shown in the schematic diagram of Fig. 1:
The *switchable amplifier/attenuator* can be used for machine studies with very high or very low bunch intensities.
The *Track&Hold amplifier* is needed to sample the top peak of each bunch pulse and freezes the value for approximately 20 ns, which is the conversion time taken by the following *analog-to-digital converter* (ADC) stage 1. As the AC-coupled inductive pickup causes a *baselineshift*, we also have to digitize the bottom value of each bunch pulse, just prior to its rising edge. Thus, Track&Hold amplifier and ADC are triggered twice per bunch, so that the difference of top and bottom pulse value leads to the baseline-shift corrected bunch intensity.

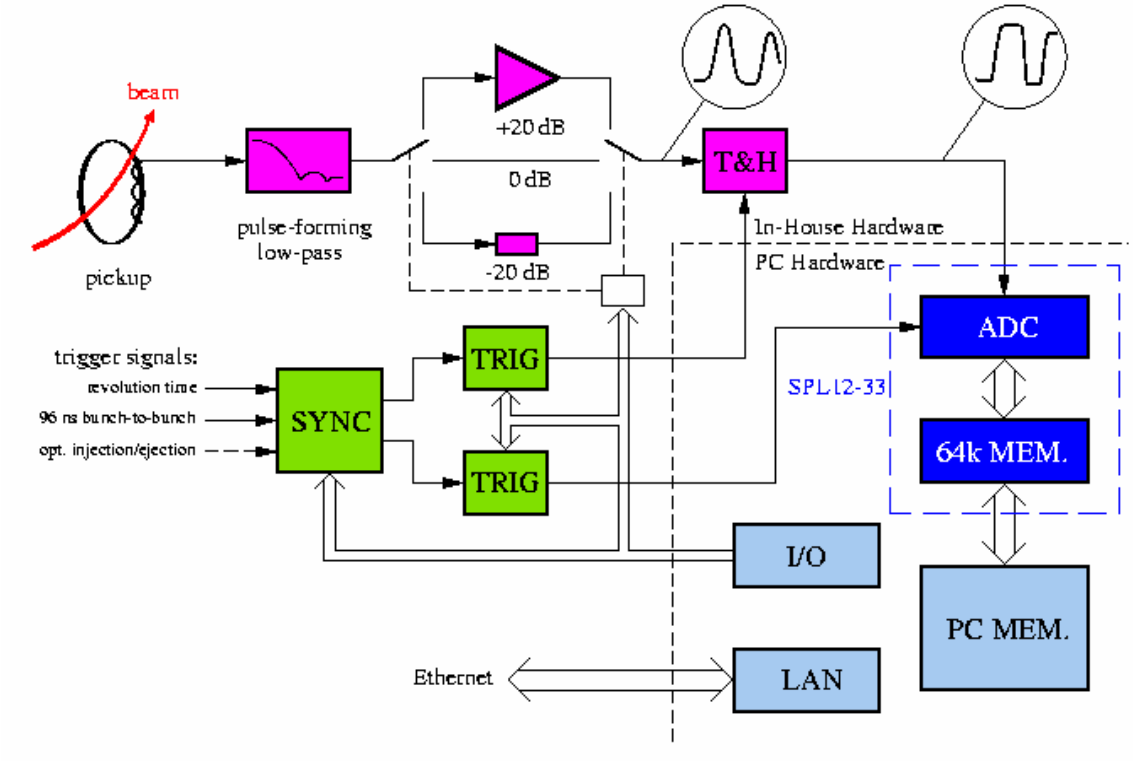

Figure 1: Schematic drawing of the hardware of the bunch current monitor

TRIGGER SIGNAL GENERATION

Trigger- (often called *clock*-) *signals* have to be supplied for the Track&Hold amplifier and for the ADC. We use external signals to realize a controlled turn-by-turn trigger scheme. All 96 ns buckets within a single turn are triggered. With an optional *injection trigger* it is possible to start the bunch current measurement on the first (or *n*th) turn after injection. The storage rings at DESY are equipped with rfsynchronous bunch and revolution *time marker systems*, which deliver two basic TTL- or NIM-level trigger signals. The *revolution trigger*, with rev.-time of the storage ring, is used as the optional injection or ejection trigger are processed in the *SYNC* and the following *TRIG* stages (see Fig. 1).
As the measurement system is controlled by a *server- PC*, we have to *synchronize* the asynchronous given M*easureOn* initializing command from the PC with the realtime revolution trigger of the bunch marker system; i.e. we always want to start the measurement with the first bunch of a turn. *MeasureOn*, which is one bit of the I/Oboard plugged on the server-PC, sets a D-FF in the *SYNC* stage. This opens a gate with the following revolution trigger pulse (see Fig. 2). Now the gate passes all following 96 ns bunch trigger pulses to both *TRIG* stages until *MeasureOn* is pulled down. In a similar manner we use the optional *injection/ejection trigger* line to synchronize the measurement for first turn data acquisition (not shown in Fig. 2).
The following *TRIG* stages, used for both, the Track&Hold amplifier and the ADC digitizer board, are nearly identical. Out of one 96 ns bunch trigger two impulses, spaced by ~30 ns, are generated for triggering the bottom and the top level of the bunch-pulse. It is particularly critical to hit (~100 ps) the peak (topvalue) of the bunch-pulse exactly. Therefore digitally controlled delay-units (type *Analog Devices AD9500*) allow fine tuning of the sampling moment for both, the top and the bottom pulse value.

SERVER-PC WITH DIGITIZER-BOARD

For the *data acquisition* and the *control* of the instrument an IBM-compatible PC is used. This server-PC is part of the accelerator's control system and sends the collected bunch current data through the LAN. Apart from the LAN-board for the network communication, the PC is equipped with a 24 channel I/O-board for various instrument control tasks. *Digitalization* and *memorization* of the analog sampled bunch pulse values are realized with a commercial plugin digitizer-board (type *Logisonic SPL 12- 33*). It was modified to DESY specifications to be *triggered* (*clocked*) externally! Equipped with the 12-bit ADC *SPT7912* it offers a 74 dB dynamic range at sufficient sampling speed (33 MS/s) and analog bandwidth (~50 MHz).
During the *data sampling* process (digitalization, *MeasureOn*- bit is set) the actual digitized data-words are first stored on the on-board memory, than mapped to the PC-memory. The digitizer-board has another DESY-modification, it is equipped with a *sample counter*. This hardware downcounter is set with the value of the initial *# of samples*, which is decremented during the sampling process with each trigger impulse. When the value reaches zero the sampling process is stopped.

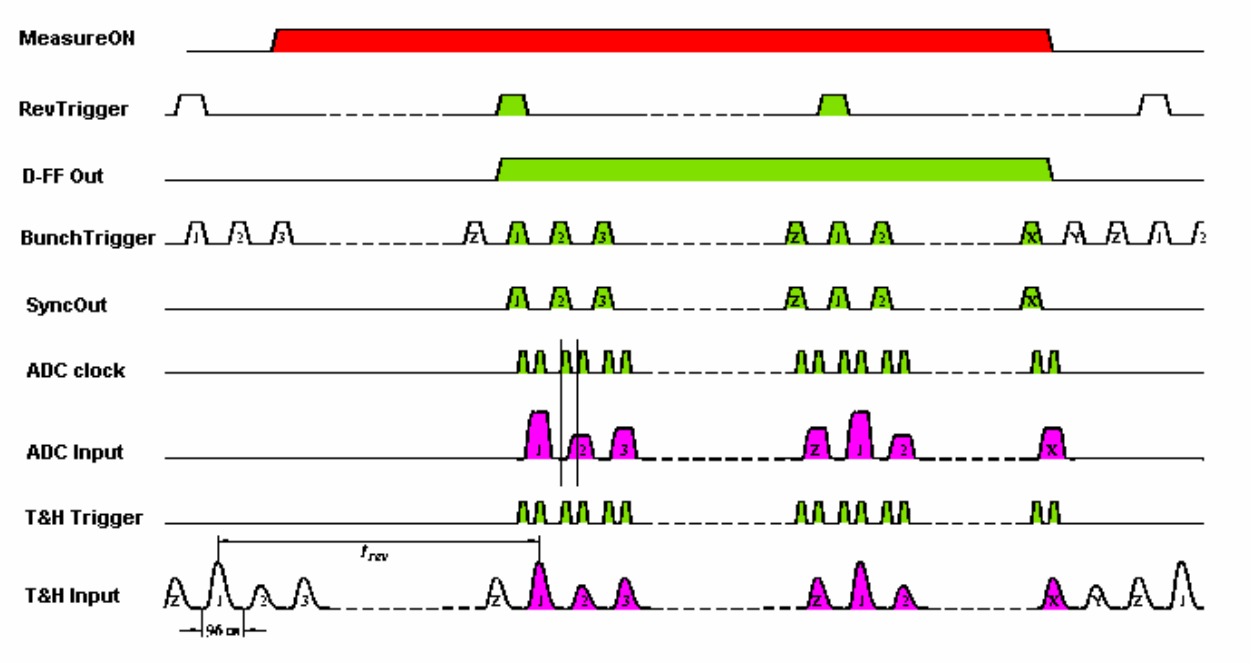

Figure 2: Timing diagram of the analog and trigger signals (buckets count 1, 2, 3, , X, Y, Z).

OPERATION AND CONTROL

The bunch current measurement system is fully controlled by the server-PC. After initialization with various default settings (board address, # of samples, _ _ _) a *measurement cycle* loop is processed. Within this loop the digitizer-board is armed and the trigger hardware is activated (load the downcounter with the # of samples, pull the *MeasureOn*-bit to *high*, etc.).
Now synchronized trigger signals – two per 96 ns bucket – sample and digitize the analog bunch current signal. With each sample the sample-counter is decreased and stops the data taking when it reaches zero. Now the server-PC takes action for data analyzing, calibration and transfer to the control system. For the operation in a ring accelerator we always initialize the sample-counter in even multiples of the accelerator's # of 96 ns buckets. In this way we analyze the bunch current of full consecutive turns and present the data as average bunch and average total current(Fig.3).

In the transport-line operation mode we analyze the *transfer efficiency* through the line. Therefore we line up the analog signals from two inductive pickups – those at the beginning and the end of the line, without signal overlapping – by using a broadband power-combiner. The samplecounter is initialized in such a way, that all bunch pulses from both pickup stations are monitored. In this mode an injection or ejection trigger impulse has to be supplied. In a similar way we line up the signals from a transport-line and a storage ring pickup to measure *injection* or *ejection efficiencies*.

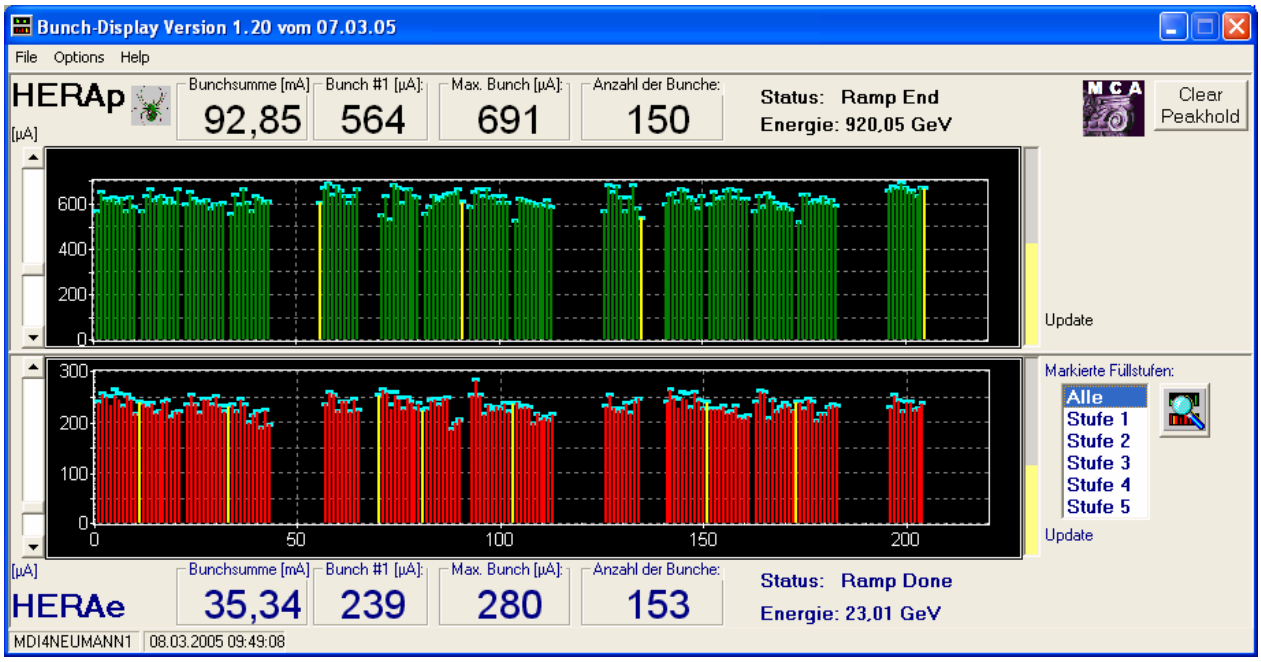

Figure 3: Hera e/p Bunchdisplay

Comparison AC – DC beam measurement for HERA p

In all DESY accelerators is the bunch intensity measurement complementary to the precision monitoring of DC-Current. Particular in the HERA-p controls the beam- and lifetimedisplay (Fig.4) includes a window for comparing DC and AC beam current. If both measurements are calibrated the difference between both devices is the unbunched beam. Comparison ACCT - DCCT is a standard technique in *HERA-p* to measure the **"coasting beam".**

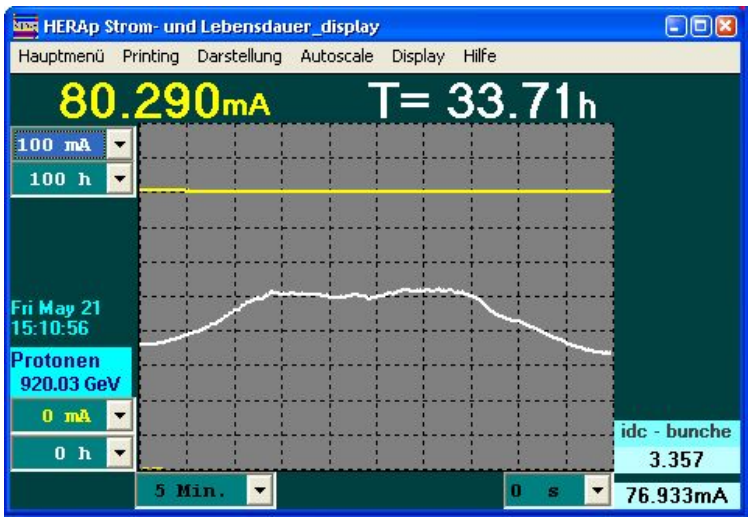

Indicator for unbunched beam

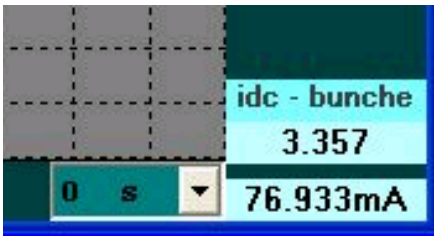

Figure 4: HERA-p DC Current & Lifetime Display

The escape of protons out of the stable RF bucket is a result of small disturbances, the major source of coasting beam for HERA-p is RF noise. Fig.5 shows a run with high coasting beam production due to RF problems; it demonstrates decreasing of total single bunch current while the DC current value remains constant.

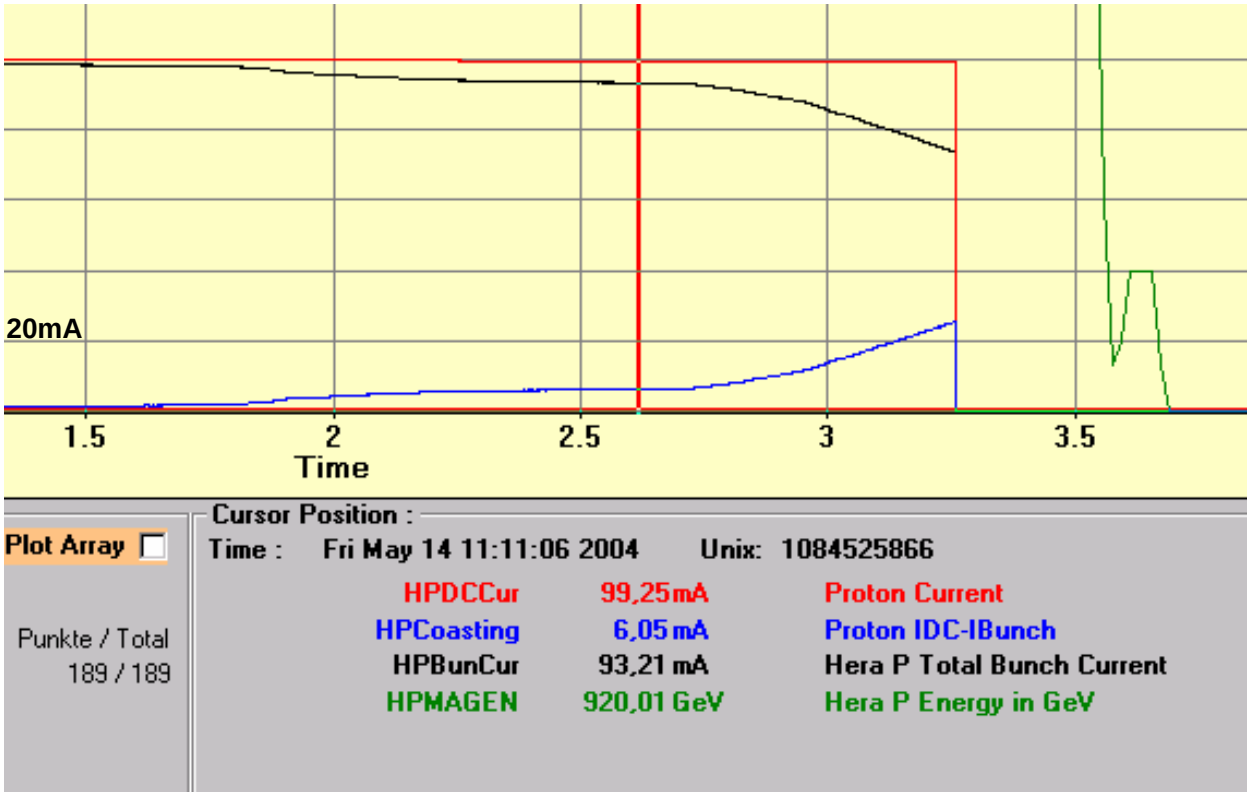

Figure 5: HERA archive reader: data for a run with high coasting beam production

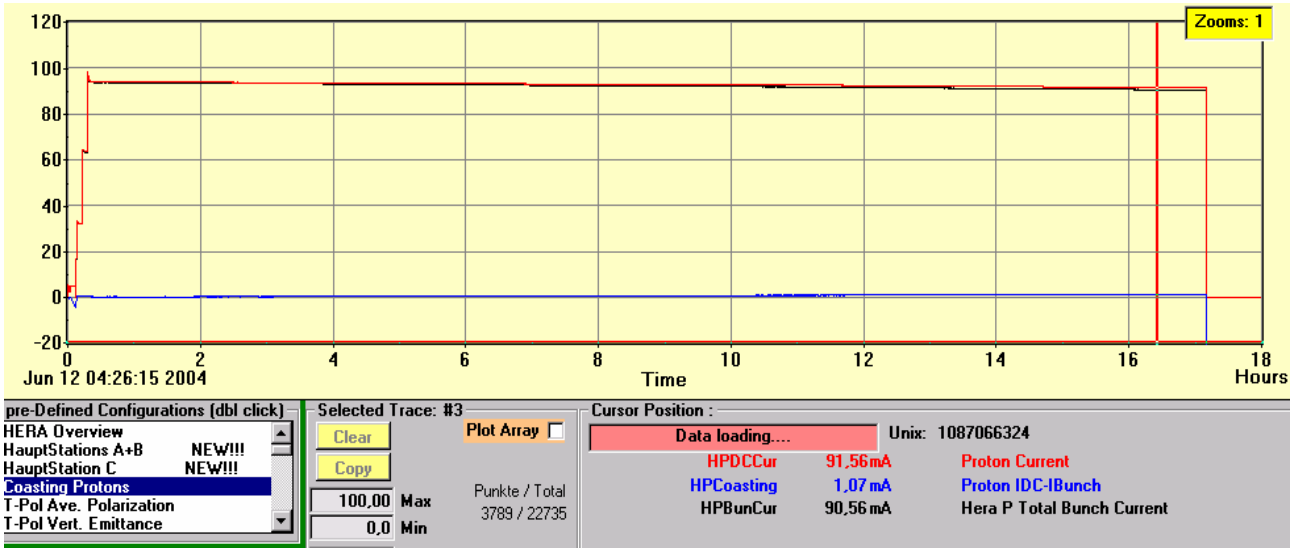

Figure 6: HERA archive reader: a normal run

Conclusions

DCCT´s from Bergoz instrumentation are

- used in most particle accelerators to measure the average beam current
- truly calibrated beam instruments for machine tuning and commissioning
- for precision measurements, they serve as a reference to calibrate other beam diagnostics

ACCT´s at DESY are used

- for single bunch monitoring
- for luminosity and backround counting in HERA experiments
- efficiency measurement between transfer lines and storage rings
- timing calibriations(kicker, first bunch

The single bunch measurement is complementary to the precision monitoring of DC current. If both are calibrated and stable in time, the difference between both devices is the unbunched beam. Comparison ACCT - DCCT is a standard technique in *HERA-P* to measure the **coasting beam.**

The New Parametric Current Transformer (NPCT)

Bergoz Instrumentation
By Klaus Unser
Presented at the 2nd CARE-N3-HHH-ABI workshop
Lyon, December 1 - 2, 2004

Motivation for a new PCT design

- The PCT was originally (1988) designed as beam current monitor for LEP. It was the 3rd Generation of the zero flux dc current transformer develop-ment which originated in CERN in 1967.
- Several key components are no longer available, including the original quality of magnetic material for the magnetic modulator
- The experience of many customers lead to a new set of specification

Requirements

- a single instrument with current ranges up to 20 A with µA resolution
- passive, radiation hard sensor, far away (up to 150 m in cable length) from the electronic hardware
- insensitive to the whole spectrum of EMC interference which are typical for an accelerator
- precise measurement of dc average current for beam signals with extreme peak to average ratios (109 : 1)
- no residual modulator frequency on output signal
- construction in standard modular crate

What is new?

- new modulator cores for operation at 30 to 40 kHz modulation frequency
- Magnet screen of sensor inside the zero flux space of the feedback winding. High values of beam currents will not magnetize the screen
- Frequency range for beam observation limited from dc to 10 kHz by the use of multiple filters to provide immunity to EMC and insure precise readings with any filling pattern in the accelerator.
- symmetrical signal transmission on a single cable between sensor and signal processing electronics
- Very high loop gain to permit gain switching over a range of 3 decades

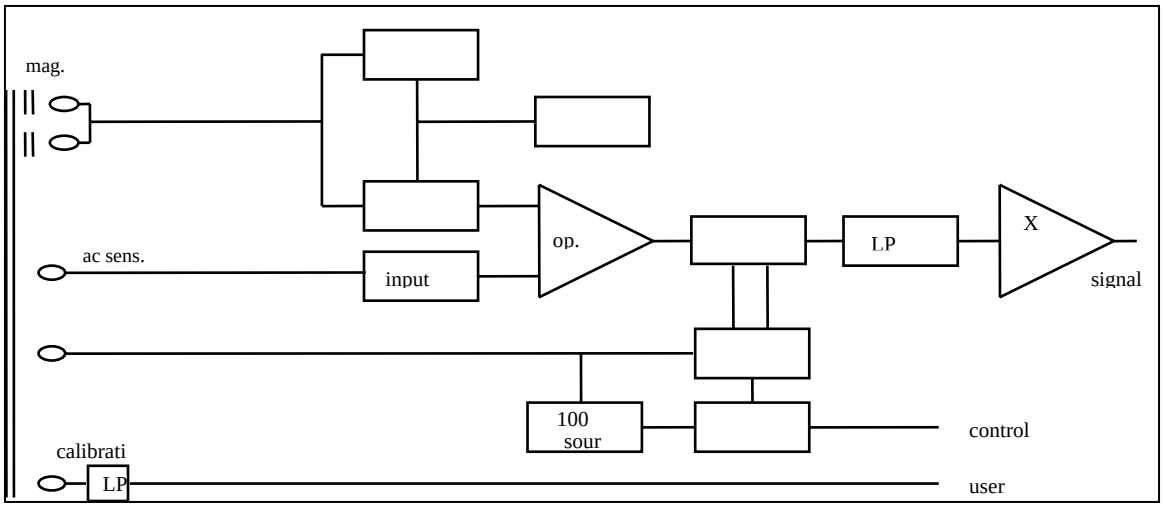

Fig. 1: NPCT block diagram (simplified)

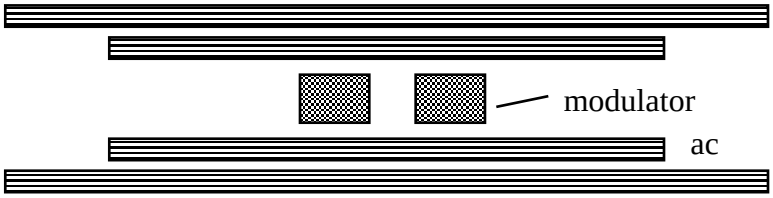

Fig. 2: Cross-section of magnetic cores in PCT sensor (drawing not to scale)

NPCT noise measurements

The SR 760 FFT Spectrum Analyser from Stanford Research Systems was used for all of the following measurements (Fig. 3-8).

The noise was recorded in 2 gain ranges for zero input current

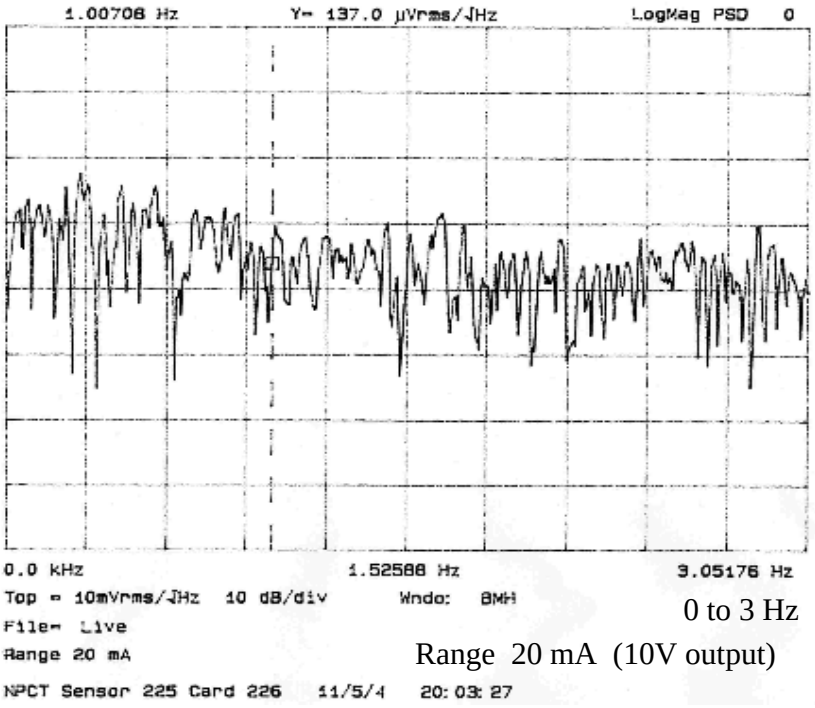

NPCT noise measurements (FFT)

Fig. 3

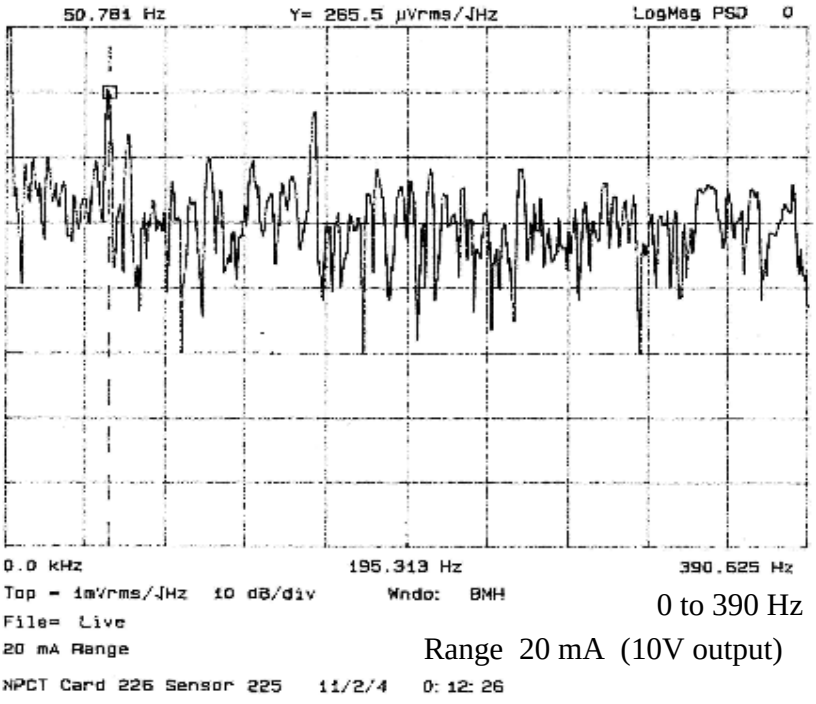

NPCT noise measurements (FFT)

Fig. 4

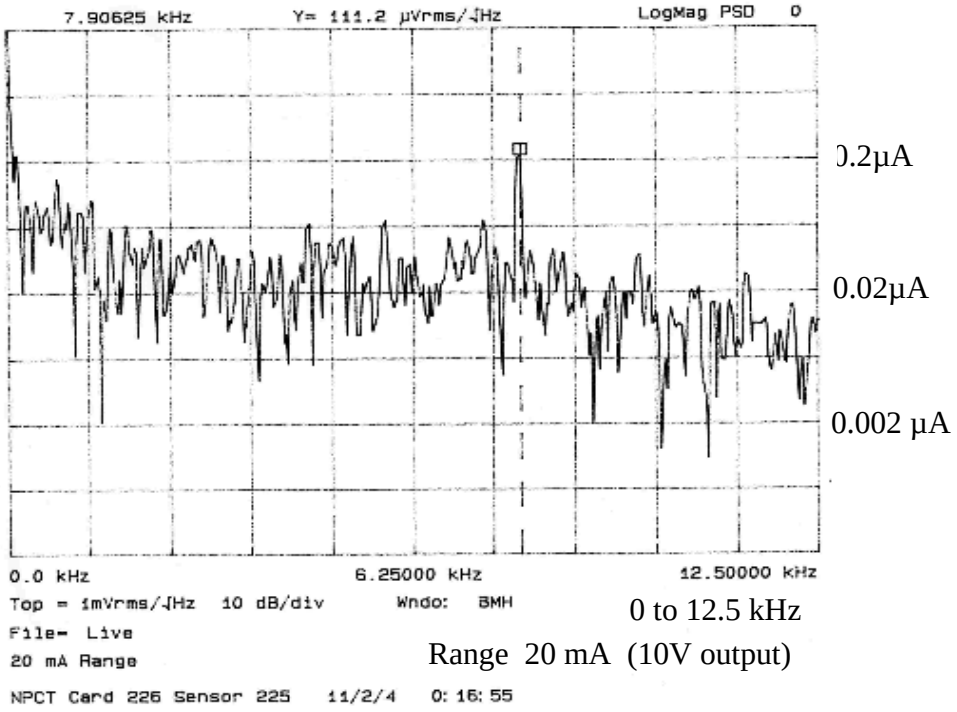

0 to 12.5 kHz

Range 20 mA (10V output)

NPCT noise measurements (FFT)

Fig. 5

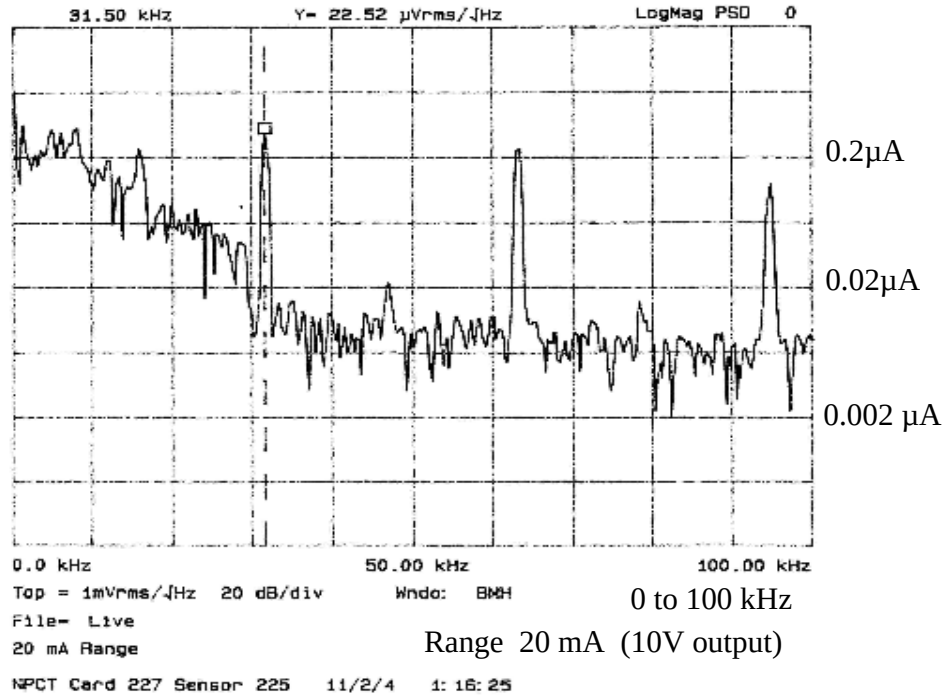

0 to 100 kHz

Range 20 mA (10V output)

NPCT noise measurements (FFT)

Fig. 6

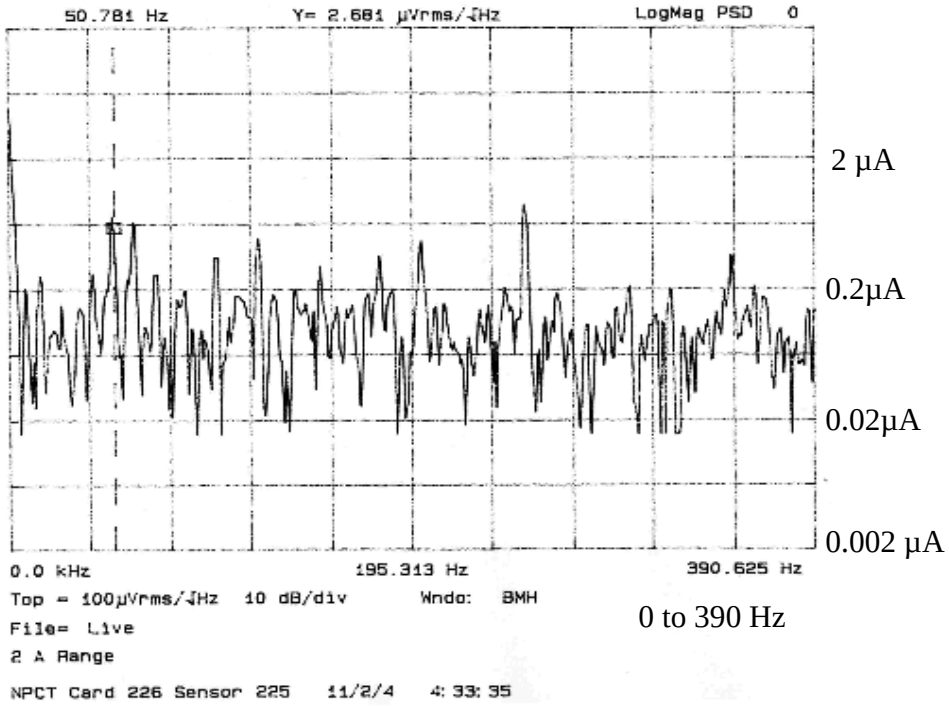

0 to 390 Hz

Range 2 A (10V output)

NPCT noise measurements (FFT)

Fig. 7

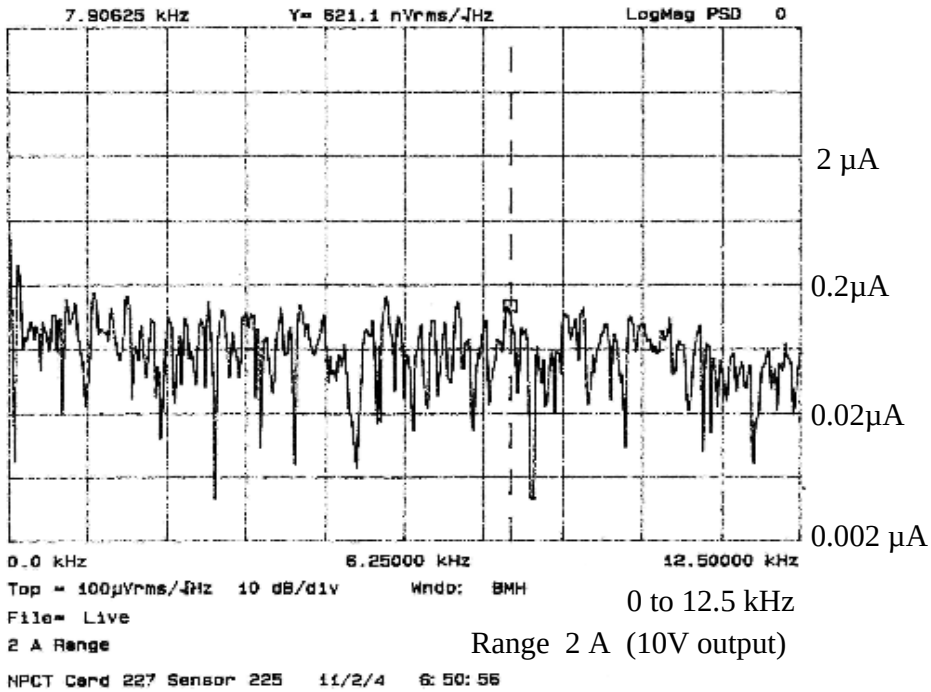

0 to 12.5 kHz

Range 2 A (10V output)

NPCT noise measurements (FFT)

Fig. 8

EUROPEAN ORGANIZATION FOR NUCLEAR RESEARCH

European Laboratory for Particle Physics

CERN - SL DIVISION

CERN SL/94-28 (BI)

REAL TIME MONITORING OF LEP BEAM CURRENTS AND LIFETIMES

A.J. Burns, B. Halvarsson, D. Mathieson, I. Milstead, L. Vos

Abstract

The data acquisition system of the LEP beam current transformers has been upgraded to provide faster monitoring of the beam currents and associated lifetimes. Two identical systems monitor separately the intensities of the 8 bunches in each beam. A simple algorithm calculates the intensity lifetime of each bunch over a variable sampling interval (between 4 s and 2 min.) that optimises the conflicting requirements of precision and fast response to changes in the lifetime. To provide instantaneous and reliable monitoring of the bunch currents and lifetimes to the machine operators, a real-time video display is generated by each data acquisition system and transmitted to TV screens in the control room. On this display, numerical values of the individual bunch currents and lifetimes and a graphical display of the recent evolution of each beam lifetime are updated at 2 Hz. At times when the accelerator is filling, the evolution of the intensity of any bunch in the seconds, milliseconds, or even individual turns following each injection replaces the lifetime history plot. The paper also includes data on the relative precision of the bunch current measurements obtained in real operating conditions and the resulting limits on the lifetime measurements that can be provided.

Paper presented at the Fourth European Particle Accelerator Conference (EPAC'94), London, United Kingdom, 27.6.-1.7.1994

Geneva, Switzerland
27th June 1994

Real Time Monitoring of LEP Beam Currents and Lifetimes

A.J. Burns, B. Halvarsson, D.Mathieson, I.Milstead, L.Vos
CERN, SL Division, CH-1211 Geneva 23

Abstract

The data acquisition system of the LEP beam current transformers has been upgraded to provide faster monitoring of the beam currents and associated lifetimes. Two identical systems monitor separately the intensities of the 8 bunches in each beam. A simple algorithm calculates the intensity lifetime of each bunch over a variable sampling interval (between 4 s and 2 min.) that optimises the conflicting requirements of precision and fast response to changes in the lifetime. To provide instantaneous and reliable monitoring of the bunch currents and lifetimes to the machine operators, a real-time video display is generated by each data acquisition system and transmitted to TV screens in the control room. On this display, numerical values of the individual bunch currents and lifetimes and a graphical display of the recent evolution of each beam lifetime are updated at 2 Hz. At times when the accelerator is filling, the evolution of the intensity of any bunch in the seconds, milliseconds, or even individual turns following each injection replaces the lifetime history plot. The paper also includes data on the relative precision of the bunch current measurements obtained in real operating conditions and the resulting limits on the lifetime measurements that can be provided.

1. INTRODUCTION

The purpose of the present paper is to describe the improved data processing performed on the LEP beam current measurements and to analyse the quality of these measurements. The hardware of the Beam Current Transformers is a upgraded version of the system described in 2 EPAC 90 papers [1,2]. Although the new system has been running since the introduction of the 8x8 bunch pretzel scheme in autumn 1992, the injection monitoring and the optimised lifetime processing described here have only been operational since the beginning of the 1994 LEP run.

2. UPGRADED BCT ACQUISITION SYSTEM

2.1 Overview

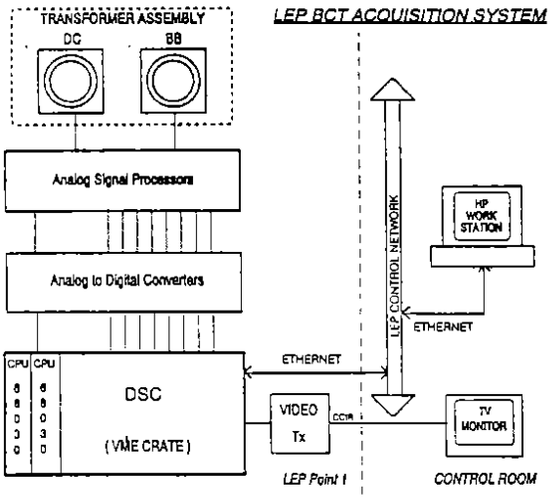

Fig. 1 : BCT acquisition system

Fig. 1 illustrates schematically the BCT acquisition system. Two such systems are used, one attached to the BCT158 for measuring e^- bunches, the other to the BCT142 for measuring e^+ bunches and the DC current. The VME acquisition cards that buffer digitisations from successive passages bunch have been modified to permit interleaved reading (by the "acquisition" CPU) and writing (from the ADCs), thus allowing the continuous acquisition of all bunch passages. The original 68010-based VME card running the RMS-68K operating system has been replaced with two 68030-based VME cards running OS-9. Additional hardware includes a video card for generating a real time display for the LEP control room and a special acquisition channel to record a timing synchronisation pulse required for the new injection monitoring facility. Communication with the control system is now via TCP-IP over Ethernet and Token Ring.

A periodic 0.5 s interrupt on the acquisition CPU triggers the readout of the last 0.5 s of turns from each ADC memory buffer. The raw data is stored in a 5 s circular buffer in the acquisition card memory that is available on request via the control system, and is also used for injection monitoring. Calibrated current averages are generated from the 5622 turns recorded for each channel and written via the VMEbus into the memory of the "master" CPU card. Finally the waiting lifetime calculation process on the master is awoken via a message sent on a RS-232 link between the 2 cards. Once the lifetime process has completed evaluating the intensity lifetimes of all bunches, it notifies the other waiting processes via an OS-9 event. The video process then updates the control room video display and a communication process sends the new current and lifetime data to a control room workstation for storage in a database and subsequent display. This sequence of processes means that, in the worst case, the data appearing on the video is 1 s old. In the original system, the processed data displayed in the control room was 5-10 s old.

2.2 Video display

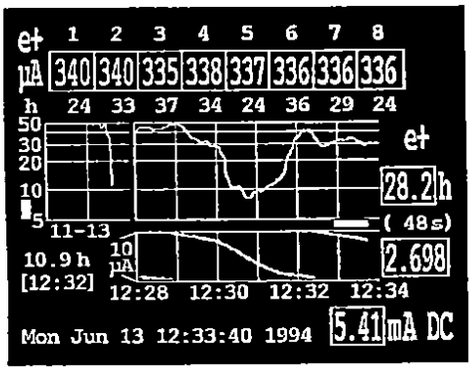

Fig. 2 : BCT video display

The colour video display (Fig. 2) has been designed to include all the intensity information from one beam needed by the operators to run LEP. At the top, the values of all 8 bunch currents (μA) and lifetimes (h) are shown. On the right hand side are the single beam lifetime (h), the interval currently used to calculate it (s), the single beam current (mA) and the DC current monitor reading (mA). In the centre are plots of the single beam lifetime on a logarithmic scale

between 5 and 50 hours (or between 0.5 and 5 h), and a 10 μA zoom of the single beam current, both during the previous 2-6 min.

All data and graphs are updated at 2 Hz, except for the small plot on the left which shows the evolution during the previous 1-2 hours of measurements of the single beam lifetime made with a fixed 128 s interval and to which a data point is added every 2 min. This plot is useful for detecting slow lifetime trends during stable conditions.

2.3 Injection monitoring

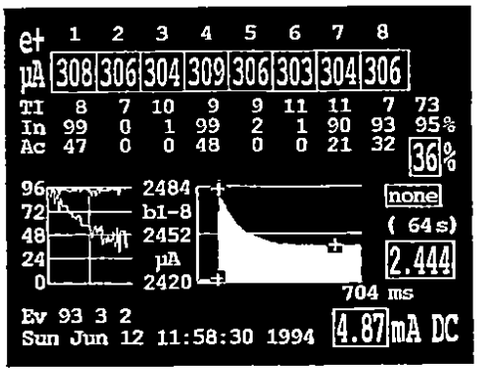

Fig. 3 : BCT video display during injection

During the injection and accumulation process, the video display changes automatically to that shown in Fig. 3. The beam currents are still updated at 2 Hz; but otherwise there is one refresh in the 2-3 s following each injection into LEP (normally every 14.4 s). Three lines of data are displayed : *TI*, the intensity (10^9 particles) measured by directional couplers at the end of each injection line; *In*, the percentage of this intensity measured as an increase in the circulating beam current about 20 turns after injection ; and *Ac*, similar to *In*, but measured about 500 ms after injection. In normal conditions, the values *Ac* then give the percentages of the injected bunch intensities accumulated in LEP.

The left hand plot shows the evolution during the last 30-60 injection cycles of the averages of *In* and *Ac* for the bunches actually injected. The other plot shows the detailed behaviour of the beam current around injection and an operator console program allows the selection of the bunch (or sum of 8 bunches) and time interval (< 5 s) to display.

This display has recently assisted in improving the accumulation efficiency from below 10% at the end of filling to the 40% seen on Fig. 3, by adjusting the trajectory of the injected beam.

3. LIFETIME CALCULATION ALGORITHM

The intensity lifetime τ is defined as that characterising an exponentially decaying beam current, $I = I_0 e^{-\tau/t}$. For sampling times $\Delta t \ll \tau$, a good estimate of τ is given by $\tau = I\Delta t / \Delta I$, where ΔI is the current change over interval Δt. To obtain the best precision, all the current values in 2 consecutive Δt intervals are averaged to calculate ΔI. There is inevitably a time lag in the response of the lifetime measurement and one should aim to use the shortest interval Δt possible, consistent with a certain level of precision on the result. The relative error on the calculated lifetime is given by $\sigma_\tau/\tau = \tau\sigma_{\Delta I}/(I\Delta t)$. Assuming random statistical errors on the 0.5 s averages (with rms value σ_I), one obtains $\sigma_{\Delta I} = \sigma_I/\Delta t^{0.5}$, where Δt is in seconds. In fact, as is discussed in section 4, the noise on the current measurements has large low frequency components, which reduces the value of the power of Δt to 0.3-0.4. Hence one obtains :

$$\sigma_\tau/\tau \sim \tau\sigma_I/(I\Delta t^{1.35}) \qquad (1)$$

For any given σ_I / I, it would be possible to use formula (1) to calculate the interval Δt corresponding to any required precision on lifetime τ. However, it is likely that the continuous variation of sampling interval would be unstable in conditions of varying lifetime. The scheme adopted instead consists of a fixed series of intervals that, for given σ_I / I, cover an overlapping set of lifetime bands. The bands are centred at the lifetime giving the required σ_τ/τ and the overlap ensures that there is no oscillation in interval selection when the lifetime is close to the edge of a band. The next higher interval is chosen when the lifetime moves above the high end of the band and the next lower interval is chosen when the lifetime falls below the low end of the band. Current sums associated with the 2 Δt intervals for each of a series of 11 intervals (2, 3, 4, 6, 8, 12, 16, 24, 32, 48, 64, 96, & 128 s) for each bunch and the bunch total are updated at 2 Hz, allowing to switch instantly from one interval to another.

When the lifetime falls, the interval is allowed to drop from one interval to the next at every acquisition (i.e. at 2 Hz). This produces a fast response to drops in lifetime. However, when the lifetime rises, a special procedure smoothly increases the interval to the next highest one at the same rate as the acquisition proceeds. This is necessary to ensure that the sampling interval is never extended backwards in time. This would result in data corresponding to lower lifetime being included and generate rapid oscillations in the interval selected and calculated lifetime. The behaviour of the lifetime algorithm is illustrated in Fig. 4 below. The dotted line on the lifetime part of the figure indicates the result that would be obtained if a fixed interval of 32 s were always used.

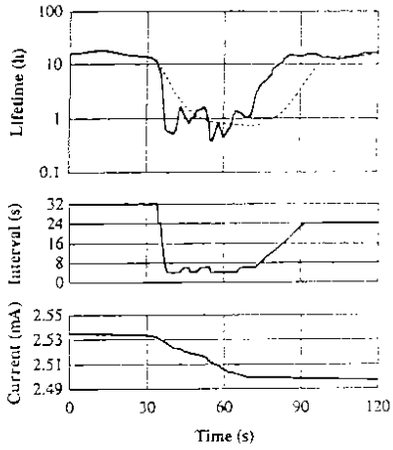

Fig. 4 : Example of application of lifetime algorithm

4. MEASUREMENT PRECISION

4.1 Noise on current values

Fig. 5 shows the variation of rms noise on individual bunch measurements, as a function of the number of consecutive beam turns averaged to produce each data point. The final points of the curves are close to the 5622 turn averages used for the lifetime measurements. The $1/\sqrt{N}$ behaviour of random statistical noise is evident on the lowest curve obtained by grounding the input of an ADC. The degree of flatness of the other curves is linked to the extent that low frequencies dominate in the noise spectra.

[3] The top curve was measured when the Beam Synchronous Timing (BST) turn-clock was still being used to generate the acquisition gates. The use of a more stable RF-based turn-clock from 1992 reduced the noise by a factor of 3. The other 2 curves represent the average of all bunch channels for a each BCT, for an

average bunch current of 250 μA, and replace the much lower BB noise curve previously published [2]. The BCT158 is seen to have twice as much noise as the BCT142 on averages from more than 2000 turns and a higher proportion of low frequencies in its noise spectrum; but as this problem is still under study, further analysis is limited to the BCT142 used for the e^+ beam.

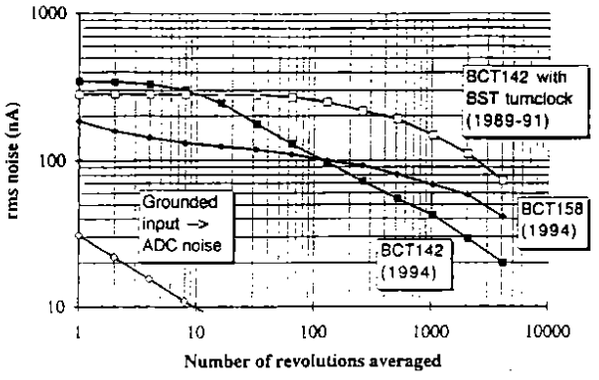

Fig. 5 : Rms noise levels as a function of the number of revolutions averaged.

The data presented in Fig. 5 are based on data samples consisting of every beam passage during 5 s. To include the effect of the sub-Hertz frequencies in the noise spectrum, constant lifetime fits were made to the 0.5 s current averages over periods of about 10 minutes when the lifetime seemed stable. The resulting standard deviation of the data about the fit included any small low frequency oscillations. That such oscillations are instrumental and not beam related had been previously verified during a run with 4 e^+ and 4 e^- bunches in which both BCTs were monitoring all 8 bunches. It was observed that there was a correlation between the slow current fluctuations seen on all bunches measured on the same BCT, but no correlation between the fluctuations observed on the same beam observed on different BCTs

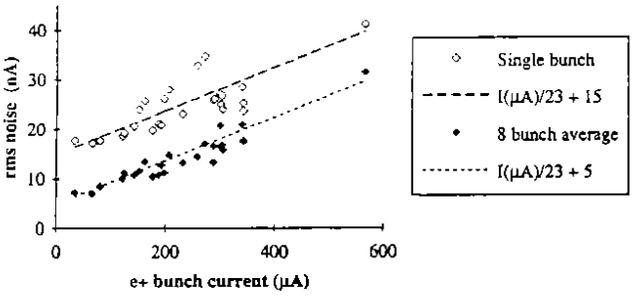

Fig. 6 : Rms noise on the 0.5 s averages as a function of e^+ bunch current

Fig. 6 shows the rms noise values resulting from the above fits as a function of bunch current for the BCT142. Plotted separately are the average of the noise values obtained from each of the 8 bunch channels and the resulting noise on the average of the 8 bunches There are two different components in the observed noise. One is random uncorrelated noise on the different electronic channels used to measure the individual bunches. This noise scales as $1/\sqrt{N}$ when the data from N channels are summed, and it dominates at low beam current (< 100 μA per bunch). The other component is highly correlated between the different channels and increases with beam current. It therefore dominates at higher beam currents. The correlated nature of this noise means that it is little reduced when the bunch channels are summed. One may identify this noise component with the "phase noise" that is generated by jitter on the integration gate and which is directly proportional to the integrated intensity [3].

The following formulae describe the observed total noise, for individual bunch channels :

$$\sigma_I \text{ (nA)} = I(\mu A)/23 + 15 \qquad (2)$$

and for the 8 bunch average :

$$\sigma_I \text{ (nA)} = I(\mu A)/23 + 5 \qquad (3)$$

For a typical beam of 8 e^+ bunches of 250 μA, σ_I is therefore about 16 nA and σ_I/I is 63 10^{-6}.

4.2 Effect on calculated lifetime

As explained in section 3, the relative error on the lifetime is kept near a fixed value by changing the sampling interval. This value of σ_τ/τ is, however, a parameter of the acquisiton system for each BCT, and may be changed for special beam conditions. The formulae (2) and (3) given above for σ_I (for e^+ only) are used to adjust in real time the lifetime bands within which each interval is selected, as the beam current changes. The result is that the higher σ_I/I at lower current is compensated by a longer interval (via formula (1)). As an illustration, Fig. 7 shows the lifetime bands used for an e^+ beam of 8 bunches to ensure $\sigma_\tau/\tau = 10\pm4\%$, for 3 different average bunch currents. The bands are labelled with the total sampling interval ($2\Delta t$, in notation of section 3) in seconds. When the lifetime is in the overlap zone between 2 intervals, the interval chosen depends on whether the lifetime is increasing or decreasing.

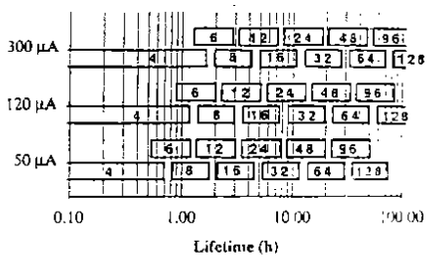

Fig. 7 : Sampling intervals versus lifetime and average bunch current for e^+ beam

5. CONCLUSIONS

The LEP BCT digital processing described in this paper now extracts the best that can be obtained from the analogue current transformer data, by acquiring all bunch passages and by adapting in real time the lifetime calculation interval to maintain the error on the lifetime within a limited range. Although the system is not able to resolve beam intensity changes of a few parts in a million in a short time interval [1], its performance has significantly improved since 1990 and is adequate for normal operation of LEP. Better performance can only come from reductions in signal noise resulting from improvements in the analogue processing, where a factor of 2 gain should be within reach [3].

6. REFERENCES

[1] K.B. Unser, "Measuring bunch intensity, beam loss and bunch lifetime in LEP", Proceedings of the 2nd European Particle Accelerator Conference, Nice, France, June 1990, pp. 786-788.

[2] G. Burtin et al., "Mechanical design, signal processing and operator interface of the LEP beam current transformers", Proceedings of the 2nd European Particle Accelerator Conference, Nice, France, June 1990, pp. 794-796.

[3] L.Vos, "The LEP monitor for the measurement of bunch intensity", CERN SL/94-18 (BI), May 1994.

LHC REQUIREMENTS TO MEASURE FAST CURRENT DROPS

R. Schmidt, CERN, Geneva, Switzerland

1. INTRODUCTION

For nominal beam parameters at 7 TeV/c, each of the two LHC proton beams has a stored energy of 360 MJ threatening to damage accelerator equipment in case of uncontrolled beam loss.

Since the beam dump blocks are the only element of the LHC that can withstand the impact of the full beam, it is essential that the beams are properly extracted onto the dump blocks at the end of a fill and in case of emergency. The time constants for failures leading to beam loss extend from μs to many seconds.

Failures must be detected sufficiently early and transmitted to the beam interlock system that inhibits injection and triggers a beam dump. Detection of failures requires the use of beam instruments (mainly beam loss monitors) and monitors to detect failures in the hardware systems.

In recent years highly efficient lifetime monitors were developed, measuring beam lifetimes of many hours within seconds. This requires very accurate measurement of the beam current with low statistical and systematic errors. In this paper the use of beam current monitors detecting a fast decay of the circulating beam current is suggested. Normally other monitors should already have detected an unsafe situation and requested a beam dump, but a beam dump after the fast detection of the beam current decay could be the last resort in case of a previously undetected failure.

2. ENERGY IN MAGNETS AND BEAMS

The LHC will provide proton-proton collisions at the centre of mass energy of 14 TeV with a nominal luminosity of 10^{34} $cm^{-2}s^{-1}$. Some parameters for the LHC as proton collider are given in Table 1. Whereas the proton momentum is a factor of seven above accelerators such as SPS, Tevatron and HERA, the energy stored in the beams is more than a factor of 100 higher. The transverse energy density as relevant factor for equipment damage is a factor of 1000 higher than for other accelerators (Table 2).

Table 1: LHC Parameters

Momentum at collision	7	TeV/c
Dipole field for 7 TeV	8.33	T
Luminosity	10^{34}	$cm^{-2}s^{-1}$
Protons per bunch	$1.1 \cdot 10^{11}$	
Number of bunches / beam	2808	
Nominal bunch spacing	25	ns

The beams must be handled in an environment with superconducting magnets that could quench in case of fast beam losses at 7 TeV of 10^{-8}-10^{-7} of the nominal beam intensity (see Table 3). This value is orders of magnitude lower than for any other accelerator with superconducting magnets and requires very efficient beam cleaning [1].

The beam intensity that could damage equipment depends on the impact parameters and on the equipment hit by the beam (Table 3).

Protection must be efficient from the moment of extraction from the SPS, throughout the LHC cycle.

3. PARTICLE LOSSES AND COLLIMATORS

The LHC requires collimators to define the mechanical aperture through the entire cycle. A sophisticated scheme with many collimators and beam absorbers has been designed [1]. Some of the collimators must be positioned close to the beam, (~6 σ). For luminosity operation at 7 TeV, the opening between two collimators jaws can be as small as 2.2 mm.

Under optimum condition the single beam lifetime could exceed, say, 100 h (Table 4). This would be very comfortable since the beam deposited power into the equipment is only about 1 kW. Still, the cleaning system should capture more than 99 % of the losses. If the lifetime decreases to 10 h, the collimators should capture more than 99.9 % of the beam losses. The collimation system is designed to accept a lifetime of about 0.2 h for a 10 s long transient, e.g. when changing the betatron tune. This corresponds to a power deposition of 500 kW. If the lifetime becomes even smaller, in particular after equipment failure, the beams will have to be dumped immediately. Depending on the type of failure, dumping the beams must be very fast.

Table 2: Energy stored in magnets and beams

Energy stored in one beam	360	MJ
Average power, both beams	~10	KW
Instantaneous beam power, both beams	7.8	TW
Energy to heat and melt one kg copper	700	kJ

Table 3: Bunch intensities, quench and damage levels

Intensity one “pilot” bunch	$5 \cdot 10^{9}$
Nominal bunch intensity	$1.1 \cdot 10^{11}$
Nominal beam intensity, 2808 bunches	$3 \cdot 10^{14}$
Nominal batch from SPS, 216/288 bunches	$3 \cdot 10^{13}$
Damage level for fast losses at 450 GeV	~$1\text{-}2 \cdot 10^{12}$
Damage level for fast losses at 7 TeV	~$1\text{-}2 \cdot 10^{10}$
Quench level for fast losses at 450 GeV	~$2\text{-}3 \cdot 10^{9}$
Quench level for fast losses at 7 TeV	~$1\text{-}2 \cdot 10^{6}$

The design of the collimators has been optimised using carbon jaws in order to withstand a full injected batch from the SPS ($3 \cdot 10^{13}$ protons), and about 10 bunches at 7 TeV (~10^{12} protons) impacting on the jaws within μs (instant impact). For an impact during many

turns, the jaws would withstand a larger number of particles without being damaged.

Table 4: Lifetime of the LHC beams (7 TeV, nominal intensity)

Beam lifetime	Lost beam power (one beam)	Comments
100 h	1 kW	Healthy operation, cleaning must work and capture >99% of the protons
10 h	10 kW	Operation acceptable, cleaning must work and capture >99.9% of the protons
12 min	500 kW	Operation only possibly for short time, collimators must be VERY efficient
1 s	330 MW	Failure of equipment - beam must be dumped rapidly
15 turns	Several 100 GW	Failure of D1 normal conducting dipole magnet - detect beam losses, beam dump as fast as possible
1 turn	~ TW	Failure at injection or by a kicker, potential damage of equipment, passive protection relies on beam absorbers

4. FAILURE SCENARIOS AND PROTECTION

Since it is not conceivable to consider all possible failures, mechanisms for particle losses are classified according to the time constant for the loss [2].

Ultrafast beam losses are losses in a single turn or less. Machine equipment is protected with collimators and beam absorbers.

Multiturn beam losses include very fast losses in less than 5 ms, fast losses in more than 5 ms and steady losses (one second or more). For multiturn beam losses any unsafe situation will be detected, a beam dump request will be issued and the beam will be extracted into the beam dump block.

Multiturn failures (fast and/ very fast losses)

Failures that could drive the beam unstable are mainly quenches of superconducting magnets and other failures in the powering system. There are operational failures and combined failures (for example after mains disturbances).

In [3] several failures were considered. A failure of D1 dipole magnets is most critical leading to a fast change of the closed orbit. Protons in the tails of the distribution would first touch collimator jaws, and more than 10^9 protons would impact on the jaw after about 15 turns. The losses would be detected by beam loss monitors. Assuming that the collimators can withstand a beam loss of about 10^{12} protons, the jaws could be damaged already after 30 turns. For dumping the beam about 10 turns (1 ms) are available. After a dipole magnet quench, the beam should be dumped within about 5 ms.

Steady losses

If the beam cleaning system captures the protons very efficiently, the heat load on the collimators might become unacceptable. Temperature monitoring of collimator jaws is planned. Beam losses and the decay of the circulating beam current (dI/dt) will be measured. If the losses are unacceptable, the beam will be dumped. If steady losses lead to an unacceptable heat load on a superconducting magnet, the magnet would quench. After a magnet quench, protection is as for fast losses discussed above.

FAILURES AND BEAM DUMP REQUESTS

For failures leading to accidental particle losses, more than one system is expected to detect the unsafe condition and request a beam dump.

Hardware diagnostics

For many systems the correct functioning of the hardware is monitored, and a beam dump request is issued in case of hardware failures.

Quench signal from Quench Protection System

When a main magnet quenches, the beam is dumped before the magnetic field decays, since it takes some time until the quench heaters become effective and the extraction switch opens,

Beam loss monitors

Beam loss monitors installed at all aperture restrictions will continuously monitor particle losses, detecting accidental beam loss within less than one turn. In general, collimators are limiting the aperture. When the emittance grows, losses will always occur firstly at collimators. For a fast growth of the closed orbit, the orbit amplitude depends on the phase between the accidental deflection and the collimators. Since the mechanical aperture at 450 GeV is only slightly larger than the collimator opening, it cannot be excluded that the beam touches another element before touching a collimator jaw.

The beam loss monitors should not only be used for protection against damage, but also to prevent quenches. Therefore beam loss monitors are also installed along the LHC arcs, together with the BLMs at aperture limitations the system covers the entire accelerator.

Magnet current change monitors

Such monitors are used for very fast detection of power converter and magnet failures. It should be possible to detect powering failures in less than one millisecond. A prototype that has been developed at CERN gave promising results [4]. A similar technique has been recently successfully implemented at HERA [5].

Beam position change monitors

To cover the full phase space, two monitors for each beam and each plane with 90 degrees phase advance are required, in total 8 BPMs. The BPMs are installed at location of high beta function, using monitors already planned to ensure maximum closed orbit amplitudes of 3.6 mm in the insertion IR6 for clean extraction into the extraction channel.

At 450 GeV, the fastest orbit movement during normal operation by an orbit corrector magnet is in the order of some mm/s. At 7 TeV the fastest movement is less than 1 mm/s. If the change of the orbit exceeds substantially this value, the beam will be dumped.

Beam current decay measurements

Beam current monitors are used as supplementary instruments to detect beam losses. The level of protection that can be achieved using a fast beam current transformer depends on the performance of the monitor and on the time constant for the beam loss. Potential damage depends where the beam hits the aperture. If the collimators are well adjusted and the protons impact on a carbon jaw, risk of damage is strongly reduced.

The damage limit of heavy materials such as copper or stainless steel is in the order of some 10^{12} protons for transient beam impact at 450 GeV, and in the order of 10^{10} protons at 7 TeV (see table 3).

A monitor that safely detects a loss of 10^{12} protons within a short time (between one turn and one millisecond) and requests a beam dump would prevent any beam induced equipment damage at 450 GeV, even if all 10^{12} particles hit the vacuum chamber in one spot. At 7 TeV, if the collimators are correctly positioned and shadowing the aperture, the carbon jaws would be hit. Depending on the impact parameters, such jaw can stand a loss of up to about 10^{12} protons without damage.

In case of beam impact outside the collimator regions, 10^{12} protons could damage vacuum chamber and possibly magnets, but more than 99% of the protons would still be extracted reducing the level of damage by more than two orders of magnitude.

If the sensitivity of the monitor would be ten times better (detection of 10^{11} protons within 1 ms), the risk of equipment damage is further reduced. It would fully protect LHC at 450 GeV and somewhat up the energy ramp. It would fully protect the LHC at 7 TeV, if carbon collimators are hit first. In the worst case, damage would be reduced by more than three orders of magnitude and therefore be limited.

The ultimate system detecting a loss of 10^{9} protons within 1 ms would protect the machine from damage under all circumstances but is currently not conceivable.

5. CONCLUSIONS

Safe operation of the LHC with high intensity beams relies on the correct functioning of several complex protection systems. Protection starts already at extraction from the SPS and collimators must define the aperture in the transfer line and in the LHC during the cycle.

For any unsafe situation, the beam must be dumped. Beam and equipment monitoring will detect such situations, e.g. in case of failures.

Fast beam current monitors would complement the protection and provide additional safety if all other detectors fail:

- Independent method to measure beam loss.
- Independent of collimators settings (although the probability for damage is strongly reduced if collimators are correctly positioned and intercepting the beams first).
- Fast for reduced accuracy (<1ms).
- Slow for high accuracy (>10ms).
- Only one instrument per beam.

It needs to be demonstrated that such a system is practical. Safety and reliability must be addressed. False beam dump triggers must be avoided.

Beam current monitors can only help for protecting the LHC against multiturn beam losses. A measurement of fast current drops cannot protect the LHC from ultra fast beam losses that require other strategies, firstly the avoidance of such losses, and secondly passive beam dilutors.

6. ACKNOWLEDGEMENTS

Several colleagues contributed to the ideas for this paper. Thanks a lot for many discussions with D.Behlorad, A.Burns, P.Odier, H.Schmickler, J.Wenninger, M.Werner and K.Wittenburg.

REFERENCES

1 R.Assmann et al., An Improved Collimation System for the LHC, EPAC 2004, Lucerne, Switzerland, June 2004

2 R.Schmidt et al., Beam loss scenarios and strategies for machine protection at the LHC, HALO '03, Montauk, NY, 19-23 May 2003

3 V.Kain, Studies of equipment failures and beam losses in the LHC, Diploma thesis, Wien, October 2002

4 M.Zerlauth et al., Detecting failures in electrical circuits leading to very fast beam losses in the LHC, EPAC 2004.

5 M.Werner, private communication

Contribution to 2nd CARE-N3-HHH-EBI meeting in Lyon, December 2004, from Pete Cameron (BNL) and Julien Bergoz (Berrgoz Instrumentation).

DIFFERENTIAL CURRENT MEASUREMENT

Julien Bergoz reported the current status of discussions and plans regarding differential measurement of two RF beams. The cases considered are those of three new projects of Energy Recovery Linacs, where the current recovery objective is 99.9995%, leading to 1 ppm resolution requirement on the current measurement. Even though these new projects are electrons accelerators, the parameters considered are fully relevant for protons accelerators, which explain why the subject was included in this 2nd CARE-N3-HHH-ABI meeting.

Parameters of the beam to be measured

Structure CW

RF 703.75 MHz

Circulating current 150, 450 and 500mA resp.

Two DC current Monitors in a differential arrangement

Some solutions were considered earlier and eliminated:

* wideband AC transformers were eliminated because their beam spectrum dependance exceed 1% (!).

* circulating the two beams through the same instrument in opposite directions was considered too difficult

The solution considered here consists of two DC monitors, one on each beam.

If the differential resolution must be in the ppm order, five significant limitations to this solution are identified:

* 1 Hz to 10 kHz magnetic cores noise

* Temperature dependence

* Magnetic field dependance

* Gain and gain linearity errors

* Beam frequency spectrum dependance

1 Hz to 10 kHz magnetic cores noise

Currently, best DC transformers have a noise density ca. 100nA/sqrt(Hz). This is based on measurements made on 30-40 pairing measurements of 20 individual cores.

It is conceivable magnetic cores noise could be reduced below 1 ppm by processing: integration, filters...

Temperature dependence

Typical temperature dependance is 5µA/K

Must be reduced to < 1ppm full scale, i.e. 0.5µA for 500mA beam current

Therefore two solutions can be retained, or a combination of the two:

* temperature stabilisation < 0.1 K

* temperature and hysteresis correction

Magnetic field dependance

Typical magnetic field dependance is 1 mA/mT, must be reduced to 0.5µA (for 500mA beam)

This poses two problems:

* a time-variable field e.g. 1mTrms must be reduced to 0.5µTrms, requiring a 2000 shielding factor

* it may be very difficult to reduce the residual field to such low value, as the magnetic permeability gets lower when the field gets lower.

Gain & gain linearity errors

Depend on the current to be measured

Can be high: ‰ 1ppm/mA, i.e. 500 ppm over 500 mA beam current range !

These errors are mainly caused by burden resistors, but not only: Other components contribute to these errors too. The gain & gain linearity errors can be near-eliminated by nulling the current flowing in the monitors. Proposed solution is a compensating current loop passing thru both monitors, to maintain the sum current seen by the monitors close to zero.

Beam spectrum dependance

The two beams have different bunch lengths. Their frequency spectra are different, and will cause different eddy current loss in their respective monitors.

Beam frequency spectrum dependance remains to be analysed.

Conclusions

Measuring 1 ppm difference current between two stable beams seems possible with state-of-the-art DC current monitors. But many questions must still be resolved:

* Magnetic cores noise processing

* Magnetic shielding

* Temperature stabilisation or correction

* Frequency spectrum dependance

Magnetic beam current measurement of high dynamics by means of optimised magneto-resistance (MR) sensor engineering in the GSI-FAIR project (facility for antiprotons and ion research)

Markus Häpe, University of Kassel, Department of Electrical Engineering and Computer Science, Measurement Engineering, Prof. Dr. W.-J. Becker, D-34109 Kassel, Germany

Introduction

The department of Measurement Engineering at University of Kassel caught attention of GSI with the development of a sensor by Mr. Barjenbruch ten years ago.

The sensor acts as a magnetic controlled oscillator with an amorphous micro strip. It has been reconstructed according to an idea of Mr. Barjenbruch. After the current state of knowledge the sensor is based on the principle of the GMI-effect.

Basic idea

The sensor will be designed in form of a “clip-on” amperemeter. This is required because of operating conditions of the accelerator. High temperatures are needed to maintain a vacuum. Also, in case the sensor needs to be changed the accelerator must not be opened.

The sensor is frequency dependent. The operating point has to be stabilised. The flux concentrator consists of a soft-magnetic material. The sensor must have high dynamics and high speed to measure the high currents during the bunch operation.

Simulation of the magnetic flux concentrator

The contour plot of the absolute values of the magnetic flux for an excitation current of 10 A is shown in Figure 2. The simulation has been carried out within a final year project at GSI. The results are used for the clip-on amperemeter within this research.

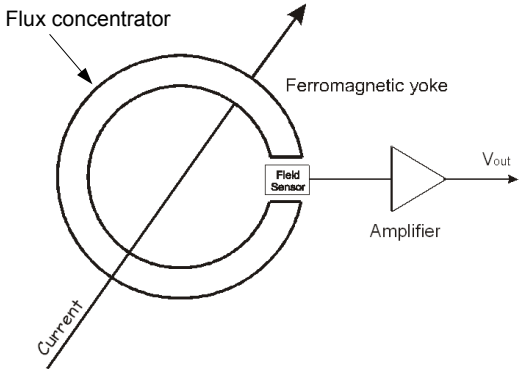

Figure 1: The open loop sensor [5]

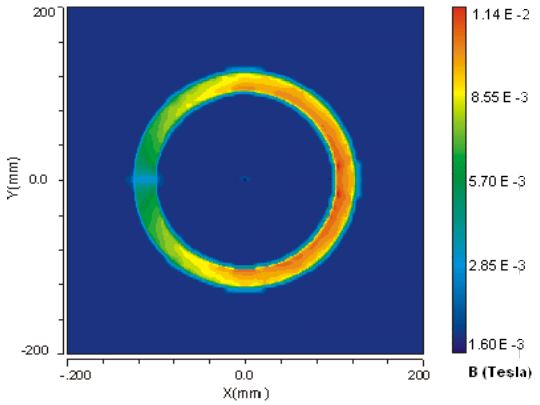

Figure 2: contour plot of the magnetic flux [5]

The material of the flux concentrator is VITROVAC 6025F. The air gap of the flux concentrator is 5 mm.

Principle Investigations on commercial MR-Sensors

Firstly the AMR and GMR sensor characteristics were determined. The characteristics have been measured in the range of +/- 4mT (Figure 3). Sensor characteristics like hysteresis, linearity and sensitivity have been measured within the magnetic field of a Helmholtz coil.

Secondly the lowest detectable value (S/N) will be determined. Therefore the 1/f-noise, the Barkhausen noise and the thermal noise from the sensor and the flux concentrator need to be detected. It is also necessary to measure the bandwidth of the sensor.

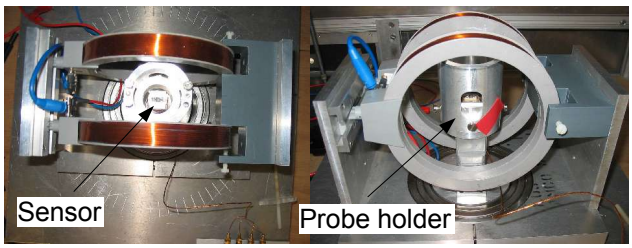

Figure 3: Sensors in the field of Helmholtz-coils

Evaluation of sensors

The sensors have been examined under laboratory conditions. Five AMR-sensors have been tested within different external electrical circuit. The first three sensors used a set- or reset- pulse to measure correctly. The remaining two sensors used a stabilisation field.

AMR-sensors:
Honeywell: HMC1001
HL PLANAR: KMY20S, KMY20M
Philips: KMZ10A, KMZ43T

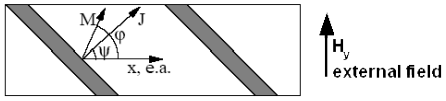

Figure 4: AMR-sensor stripe with Barberpole structure [3]

Magnetoresistive effect of an AMR-sensor stripe:

$$R(\Theta)=R+\Delta R\cdot cos^2(\Theta) \qquad \Theta=\varphi-\psi$$

Two GMR-sensors were measured. The first is an absolute measurement sensor, the second is a differential sensor.

GMR-sensors:
NVE: AA002, AB001

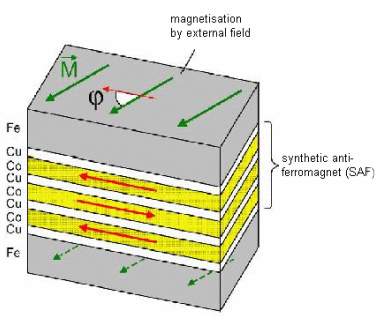

Figure 5: Structure of a GMR-multilayersensor [6]

The investigated sensors were based on a GMR-multilayer system.

AMR-sensor characteristics

The measured characteristics compared well with the data sheet characteristics. It shows that the sensor characteristics can be determined with the measuring system.

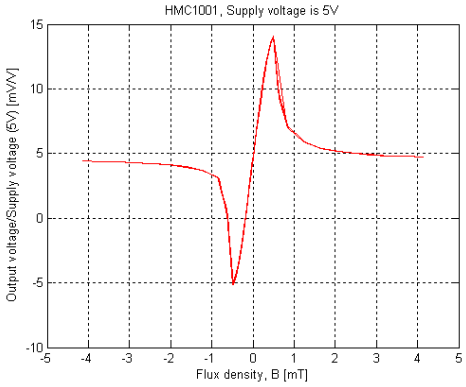

Figure 6: Measurement characteristics of HMC1001

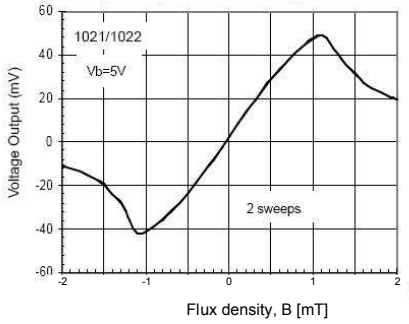

Figure 7: Data sheet characteristics of HMC1001 [1]

GMR-sensor characteristics

The measured characteristics compared well with the data sheet characteristics. It also shows that the sensor characteristics can be determined with the measuring system.

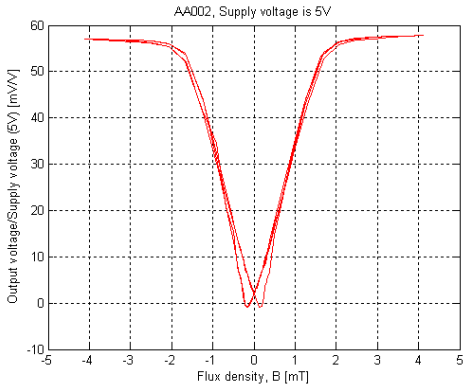

Figure 8: Measurement characteristics of AA002

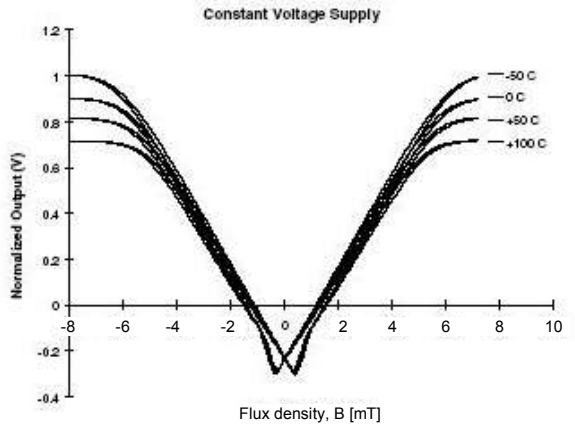

Figure 9: Data sheet characteristics of AA002 [2]

Summary of the AMR and GMR measurement

The measurement results show that the characteristics were reproducible.

Nevertheless, some mesurement problems can occur when using the sensors. The usage of the stabilisation field, set- and reset- pulse, limitations of commercial sensors and the difficult orientation in the “clip-on” amperemeter can have effects on the reproducibility of the measured values.

Sensor	Measuring range	Sensitivity	Nonlinearity	Hysteresis
HMC1001 AMR [1]	±0,159 $\frac{kA}{m}$	31,4...50,3 $\frac{mV/V}{kA/m}$	1%	0,05%
AA002 GMR [2]	1,194 $\frac{kA}{m}$	37,7.....52,8 $\frac{mV/V}{kA/m}$	2%	4%
Source:	[1] Data sheet, Honeywell, HMC1001/HMC1002 [2] Data sheet, NVE, AA002-AA006 Series			

Table 1: Table technical data from data sheets [1,2]

Resolutions of 10^{-10} T for AMR and 10^{-13} T for GMR can be obtained with optimised sensor strips on best laboratory conditions [4].

Magnetic controlled oscillator (MCO)

The sensor is a magnetic controlled oscillator which uses the GMI-effect to tune the oscillator frequency. These sensors are called GMI-sensors.

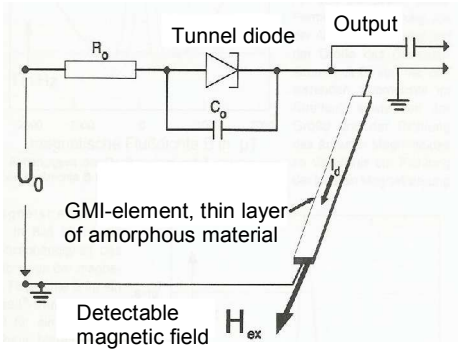

Figure 10: Principle structure of the sensor [7]

Technical data [7]:

- 3,5 mm up to 10 mm length (sensitivity increases with length)
- 100 µm width
- R_0 is the entire real part of the circuit impedance
- C_0 is the entire part of circuit capacity (~50 pF)

GMI-sensor characteristics

The frequency components of the oscillator were measured with a spectrum analyser.

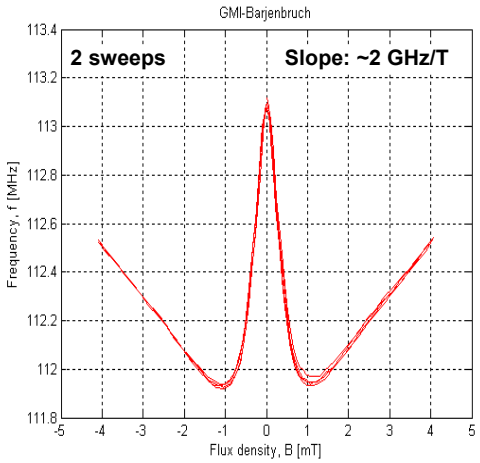

Figure 11: Measurement characteristics of the GMI modulated MCO

Investigations have shown that the GMI-stripe is suitable for measurements within a range of ±1 mT. The frequency modulation caused by GMI achieves a peak frequency deviation of 1 MHz. The oscillator frequency is 113,1 MHz.

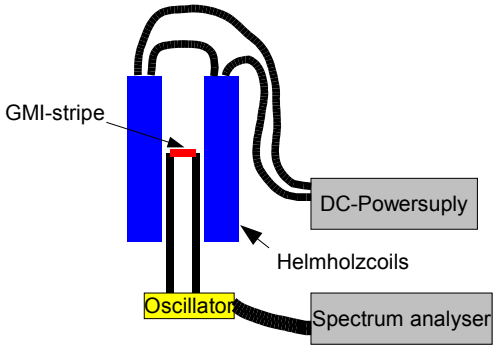

Figure 14: Principle structure of the measuring system with the MCO

The magnetic operating point of the GMI-sensor needs to be optimised and the magnetic saturation effect needs more investigation. The EMC (Electromagnetic compatibility) has to be checked. The signal of the GMI-sensor is detected by spectral analysis. The frequency of the GMI-sensor has to be stable. The geometry, the contact and the material of the amorphous wire have to be specified.

Further proceeding, questions and discussion

Further examinations will involve dynamic field measurements. Therefore a construction of a simulation device with a 50 ohm cable impedance will be constructed.

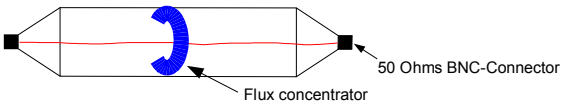

Figure 12: Drawing of the simulation device

After the measurements with the sensors have been done, a suitable sensor principle has to be selected. More information about the GMI-effect can be found in the master thesis “Investigation of the GMI-effect and an estimation of the use for the beam current measurement”.

Summary

The beam current measurement with high dynamics by means of MR sensors in “clip-on” amperemeter design. Capability study of the GMI-effect for the measurement of the beam current. Selection of the suitable sensor types.

References

[1] Data sheet, Honeywell, HMC1001/HMC1002
[2] Data sheet, NVE, AA002-AA006 Series
[3] Dr.-Ing. Werner Ricken: *Wegmessung mit magnetoresistiven Sensoren*, Kassel, Februar 2001
[4] Mengel, S.: *Technologie-Früherkennung, Technologieanalyse Magnetismus*, Band 2, XMRTechnologie, Hrsg.: VDI Technologie-zentrum Physikalische Technologien, Düsseldorf, 1997
[5] Natalya Miski-Oglu: *Simulation of the magnetic field distribution in a toroidal magnetic flux concentrator,* Diploma Thesis, Darmstadt 2004
[6] Prof. Dr. Rudolf Gross / Dr. Achim Marx: *Grundlagen der Magnetoelektronik - Vorlesungsskript zur Vorlesung im WS 2000/2001*, Walther-Meissner-Institut, Lehrstuhl für Technische Physik (E23), Garching, 2000.
[7] Dr. rer. nat. Ullrich Barjenbruch: *A novel highly sensitive magnetic sensor*, Sensors and Actuators A, 1993, 37-38, 466-470

Round table discussion and Spontaneous Presentations

Data and results of lifetime algorithm comparisons

all

Dear colleagues
As you are announced to join our 2nd CARE Meeting in Lyon, you might be interested to help us for the second half day (Topic: Lifetime algorithm):
The operators in the control room want so see a stable lifetime display, even for lifetimes in the order of some hundreds hours, as well as they want to observe fast drops and recoveries. This is somehow a contradiction and we are interested in your solution.
Maybe we can find the best suited and for the future a common solution for Lifetime algorithm (worldwide?).
Attached you will find a comma separated value file (MessungASCII_041107_031038.csv) with some data collected during a DORIS run on July 8 2004. In the first row you will find the beam current in mA, the second row is the UNIX Time in seconds.
More:
About 10 hours lifetime, 20000 data samples taken at about 5 Hz.
To compare lifetime algorithms, "events" have been added to the data: a sudden drop in the lifetime and then recovery, a sudden loss of beam, and spikes.
It would be very interesting, if you will present us your algorithm results based of our data, just to compare and to discuss it during the session. A few slides are really welcome.
If you have any question, Marc (Mark.Lomperski@desy.de) is glad to answer.
The Figures 1-4 are results from LEP lifetime algorithm based on the DESY data, kindly elaborated by A. Burns (CERN)

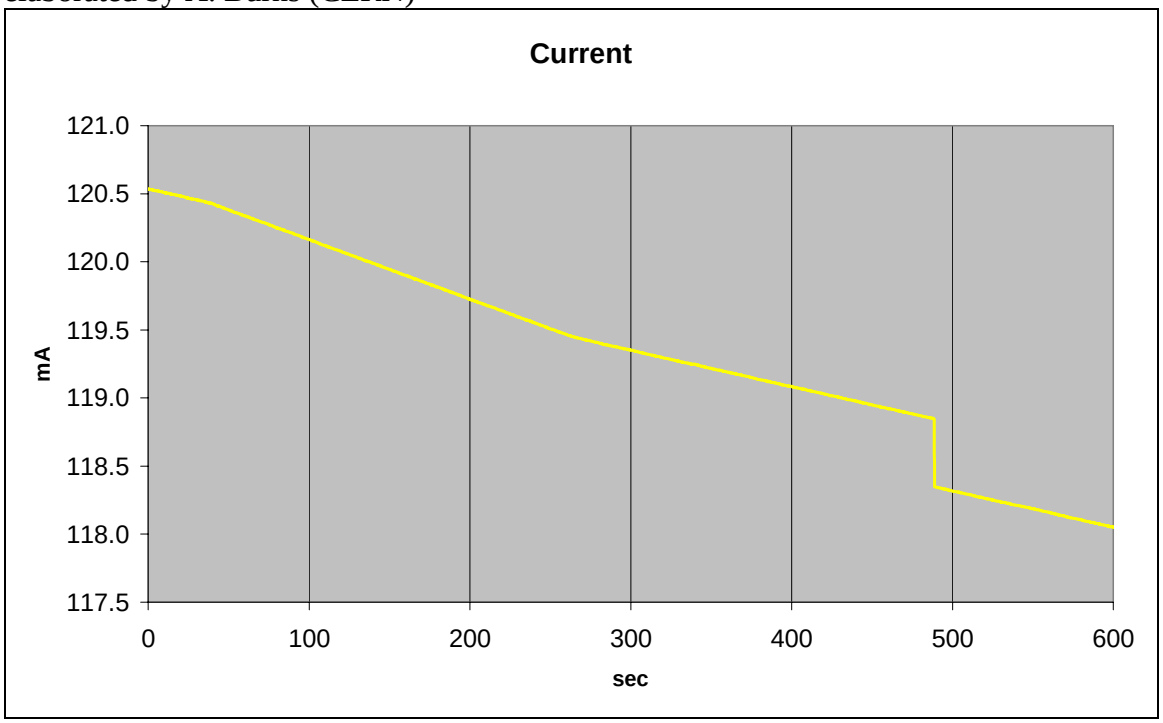

Fig. 1. Beam current data measured at DORIS (DESY)

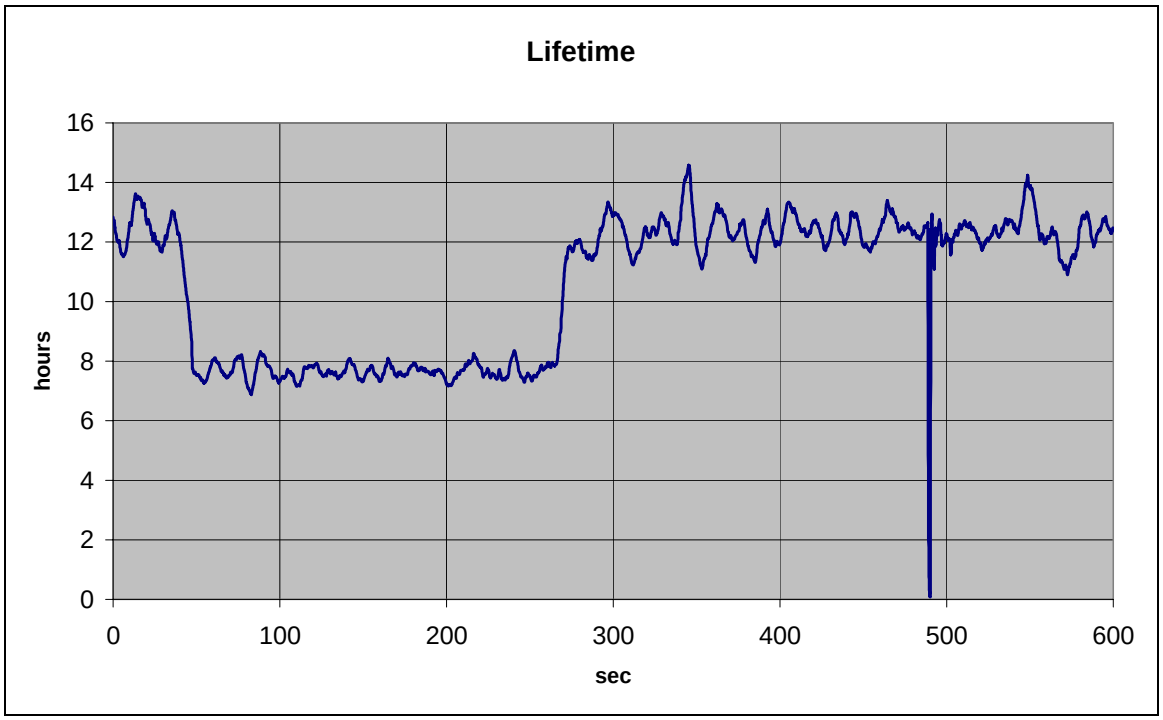

Fig. 2: Calculated lifetime by A. Burns

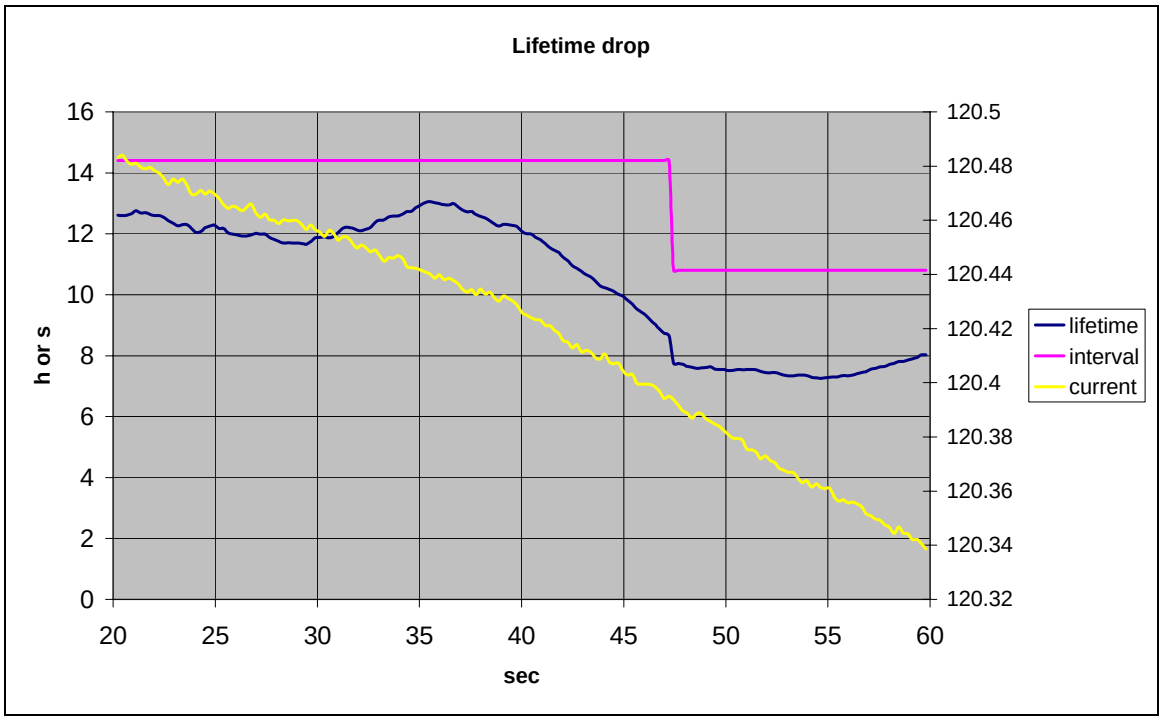

Fig. 3: first drop

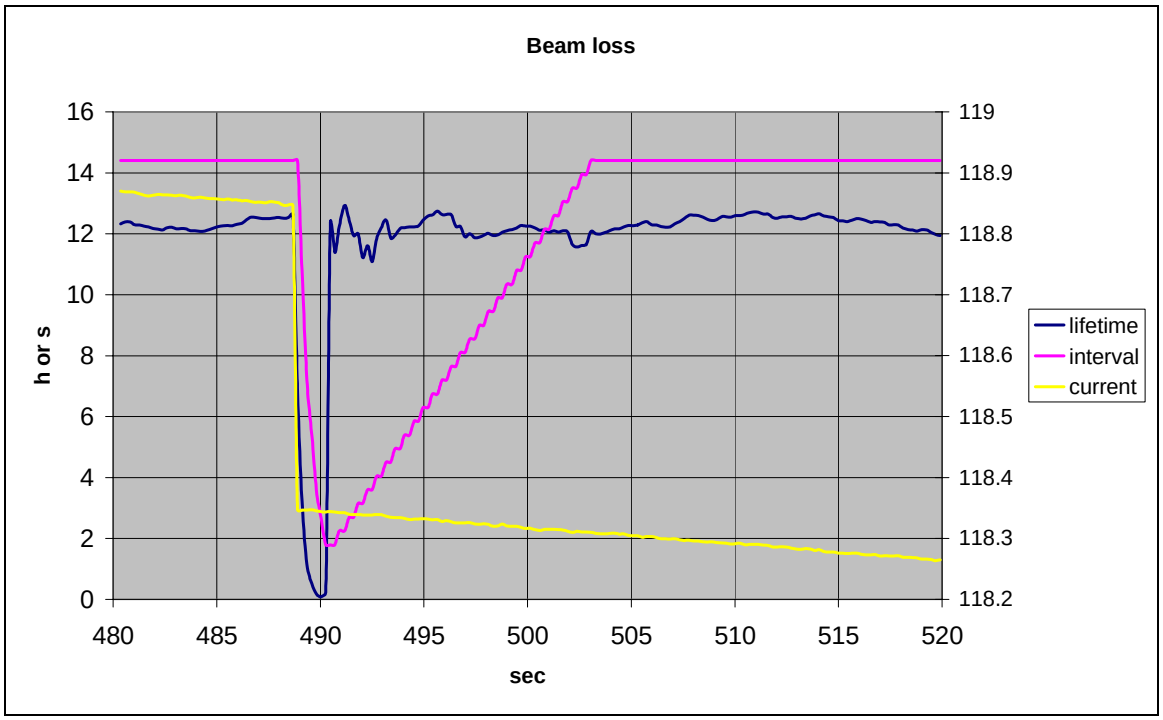

Fig. 4 second drop (beam loss)